



Article

Ecotoxicity to Freshwater Organisms and Cytotoxicity of Nanomaterials: Are We Generating Sufficient Data for Their Risk Assessment?

Tatiana Andreani ^{1,2,3,*}, Verónica Nogueira ⁴, Ana Gavina ³, Saul Fernandes ³ , José Luís Rodrigues ⁵, Vera V. Pinto ⁵, Maria José Ferreira ⁵, Amélia M. Silva ^{2,6} , Carlos M. Pereira ¹ and Ruth Pereira ^{3,*}

- ¹ Centro de Investigação em Química da Universidade do Porto, CIQUP & Department of Chemistry and Biochemistry, Faculty of Sciences of the University of Porto, Rua do Campo Alegre, 4169-007 Porto, Portugal; cmpereir@fc.up.pt
 - ² CITAB—Centre for Research and Technology of Agro-Environmental and Biological Sciences, University of Trás-os-Montes e Alto Douro, UTAD, 5000-801 Vila Real, Portugal; amsilva@utad.pt
 - ³ GreenUPorto—Sustainable Agrifood Production Research Centre & Department of Biology, Faculty of Sciences of the University of Porto, Rua do Campo Alegre s/n, 4169-007 Porto, Portugal; ana.gavina@fc.up.pt (A.G.); saulsimao@gmail.com (S.F.)
 - ⁴ Interdisciplinary Centre of Marine and Environmental Research (CIIMAR), University of Porto, Terminal de Cruzeiros do Porto de Leixões, Av. General Norton de Matos s/n, 4450-208 Matosinhos, Portugal; veronica.nogueira@fc.up.pt
 - ⁵ Centro Tecnológico do Calçado de Portugal, Rua de Fundões—Devesa Velha, 3700-121 São João Madeira, Portugal; jose.rodrigues@ctcp.pt (J.L.R.); Vera.pinto@ctcp.pt (V.V.P.); MJose.Ferreira@ctcp.pt (M.J.F.)
 - ⁶ Department of Biology and Environment, University of Trás-os-Montes e Alto Douro, UTAD, Quinta de Prados, P-5000-801 Vila Real, Portugal
- * Correspondence: tatiana.andreani@fc.up.pt (T.A.); ruth.pereira@fc.up.pt (R.P.); Tel.: +351-220-402-000 (T.A. & R.P.)



Citation: Andreani, T.; Nogueira, V.; Gavina, A.; Fernandes, S.; Rodrigues, J.L.; Pinto, V.V.; Ferreira, M.J.; Silva, A.M.; Pereira, C.M.; Pereira, R.; et al. Ecotoxicity to Freshwater Organisms and Cytotoxicity of Nanomaterials: Are We Generating Sufficient Data for Their Risk Assessment? *Nanomaterials* **2021**, *11*, 66. <https://doi.org/10.3390/nano11010066>

Received: 30 November 2020
Accepted: 22 December 2020
Published: 30 December 2020

Publisher's Note: MDPI stays neutral with regard to jurisdictional claims in published maps and institutional affiliations.



Copyright: © 2020 by the authors. Licensee MDPI, Basel, Switzerland. This article is an open access article distributed under the terms and conditions of the Creative Commons Attribution (CC BY) license (<https://creativecommons.org/licenses/by/4.0/>).

Abstract: The aim of the present study was to investigate the eco-cytotoxicity of several forms of nanomaterials (NM), such as nano-CuO, nano-TiO₂, nano-SiO₂ and nano-ZnO, on different aquatic species (*Raphidocelis subcapitata*, *Daphnia magna* and *Lemna minor*) following standard protocols and on human cell lines (Caco-2, SV-80, HepG2 and HaCaT). Predicted no-effect concentrations (PNEC) or hazard concentrations for 5% of the species (HC₅) were also estimated based on the compilation of data available in the literature. Most of the NM agglomerated strongly in the selected culture media. For the ecotoxicity assays, nano-CuO and nano-ZnO even in particle agglomeration state were the most toxic NM to the freshwater organisms compared to nano-TiO₂ and nano-SiO₂. Nano-ZnO was the most toxic NM to *R. subcapitata* and *D. magna*, while nano-CuO was found to be very toxic to *L. minor*. Nano-CuO was very toxic to Caco-2 and HepG2 cells, particularly at the highest tested concentrations, while the other NM showed no toxicity to the different cell lines. The HC₅ and PNEC values are still highly protective, due to data limitations. However, the present study provides consistent evidence of the potential risks of both nano-CuO and nano-ZnO against aquatic organisms and also their effects on public health.

Keywords: metal oxide nanomaterials; toxicity; *Raphidocelis subcapitata*; *Daphnia magna*; *Lemna minor*; human cell lines; PNEC; HC₅; risk assessment

1. Introduction

The industrial applications of nanomaterials (NM) have gained great significance by increasing the efficacy and stability of several market products [1,2]. Nevertheless, apart from the rapid advent of nanotechnology in a large number of industries, the toxicity of these new entities is still unknown and there is a general apprehension in society regarding the human and environmental risks associated with NM exposure [3]. The concern is

not only about the possible toxic effects of NM on human health during the use of NM-containing products but also the impact on ecosystems at the end of their lifecycle and after the disposal of nano-based products in the environment [4–6]. In fact, although some products containing NM are currently available in the market, information about their toxicological data are only now emerging.

NM can be released from manufactured products into water resources during the manufacturing processes, during their life through usage and washing and/or by the elimination of the products at the end of their lifecycle [7–9]. The effects of these products containing NM on public health and biota (aquatic/terrestrial organisms) during their lifecycle are inevitable and thus it is essential to assess what these effects are.

The diversity of NM and their physicochemical properties, as well as their behavior under environmental conditions, are the reason for several knowledge gaps. Although there are numerous studies correlating the impact of NM with their physicochemical properties (e.g., particle size, surface charge, surface coating, shape and ion dissolution) [10–14], most *in vitro* and *in vivo* data from NM toxicity assessments are contradictory, since toxic and non-toxic effects are often reported apparently for the same NM (for example, nano-TiO₂), but, in fact, the great majority of studies were conducted with different NM (e.g., nano-TiO₂ can be commercially acquired or synthesized in the lab; it can be in anatase or in rutile form, it can have different particle size/surface charge/morphology, and it can be functionalized or not). Therefore, the conclusions about the hazardous nature of NM are poorly supported and/or frequently reported as ambiguous due to the wide variety of NM types being tested. Additionally, changes in NM physicochemical properties, when exposed to a particular aqueous medium, may lead to the formation of agglomerates/aggregates in aqueous suspensions, especially in those with high ionic strength, which may alter the toxicological profile.

Most existing data concerning the toxicity of NM show a size-dependent effect, in which toxicity increases with decreasing particle size [15,16]. Small particles possess higher surface area-to-volume ratio in comparison to larger particles, leading to an expected increase in particle reactivity and toxicity. However, considering that NM can form agglomerates/agglomerates when dispersed into high-ionic-strength solutions (e.g., culture media) [17,18], as well as in the presence of organic matter [19], the agglomeration state of NM should not be neglected in toxicity testing. For example, the evaluation of the toxicity of NM dispersed in aqueous suspensions, or in a particular organic solvent that presents low values of average particle size and low polydispersity index, may not be representative of the state of NM in real environmental scenarios (culture media), where particle aggregation/agglomeration can occur. Several works have correlated the toxicity of NM to a particular organism or human cell line with the NM's small particle size, without evaluating their real physical properties in the exposure medium, which may lead to misinterpretation and illusion about the effects of NM. In our previous work, we showed that even in large agglomerates, metal NM (silver and copper) can be hazardous to aquatic biota and human cells at concentrations $\leq 20 \text{ mg L}^{-1}$ [17]. In this context, not only do the physical properties of each NM play an important role in the toxicological assays, but so do the chemical composition, the behavior and fate of NM under environmental conditions; and mainly the surface interactions between NM with biological membranes must also be taken into account.

Based on these considerations, the present study focuses on the characterization and the toxicity evaluation of NM widely used in consumer products, such as nano-CuO, nano-TiO₂, nano-ZnO and nano-SiO₂. Due to their biocidal characteristics, nano-TiO₂ and nano-ZnO have been extensively explored in several industrial classes of products, including medical tools, cosmetics, food and fabric coatings to control bacteria and fungi growth [20]. In addition, because of their ability to filter UV-A and UV-B radiation, nano-TiO₂ and nano-ZnO have been used in sunscreen formulations [21]. Nano-TiO₂ is also applied in toothpaste to provide whiteness and opacity [22]. Nano-CuO has great potential in thermal conductivity [23], while nano-SiO₂ is a popular anticaking agent widely used in

food products [24]. Although the literature suggests that these NM are among the most studied, an exhaustive bibliographic search has shown that, in fact, although there is a large amount of toxicity data available for NM, there are also many differences in their physical properties, as well as in the experimental conditions of toxicity assays performed to evaluate their impact on the environment and public health. The lack of coherence in toxicity data regarding NM is in part due to differences in NM within the same category (commercial versus lab-synthesized NM, and several methods of synthesis), differences in susceptibility among the test organisms/cell lines and great diversity in the experimental conditions (e.g., dispersion medium, exposure time and pH). Therefore, the present study was designed to investigate: (i) existing data for the metal oxide NM used in this study, in order to testify to the novelty of our results and to provide evidence that we are far from having sufficient data to support the risk assessment for the great diversity of NM that are being manufactured; (ii) the physicochemical properties of the different commercial metal oxide NM when suspended in the culture media of distinct test organisms in order to reflect adequately the exposure modes; (iii) the effects of NM on aquatic organisms (microalgae *Raphidocelis subcapitata*, crustaceans *Daphnia magna* and aquatic plants *Lemna minor*) and (iv) the effects of NM on human cellular lines derived from intestine (Caco-2), liver (HepG2), skin (HaCaT) and lung (SV-80), representing the main human exposure pathways.

2. Materials and Methods

2.1. Nanomaterials, Chemicals and Reagents

The commercial NM used in the present study were obtained from PlasmaChem GmbH Company (Berlin, Germany) and are listed as follows: zinc oxide powder (ZnO, particle size of 25 nm), hydrophilic TiO₂ powder stabilized by HNO₃ (TiO₂, particle size ranging from 4 to 8 nm, anatase phase), fumed hydrophilic SiO₂ nanopowder (particle size ranging from 7 to 14 nm), SiO₂ in a 30% aqueous suspension (average particle size of 10 nm) and CuO (average particle size of 40 nm).

Fetal bovine serum (FBS), Dulbecco's Modified Eagle's Medium (DMEM), antibiotics solution (composed by penicillin and streptomycin), L-glutamine, 0.05% trypsin-ethylenediamine tetraacetic acid (EDTA) solution and Alamar Blue[®] (AB) reagent were obtained from ThermoFisher Scientific[®] (Alfagene[®], Carcavelos, Portugal). Ultrapure water was produced by the Milli Q[®] water purification process (18.2 MΩ cm, Millipore, Darmstadt, Germany).

2.2. Suspensions and Characterization of NM

To verify the NM behavior under experimental conditions similar to those used in the toxicity studies, three intrinsic properties of NM were evaluated: the mean particle size, the polydispersity index (PI) and surface charge. For this purpose, the suspensions were prepared at 20 mg L⁻¹ (in respective culture media), the highest concentration used for algae *R. subcapitata* (Woods Hole MBL), *D. magna* (ASTM hard medium), *L. minor* (Steinberg medium) and human cell lines (DMEM), followed by sonication for 30 min in an ultrasonic bath (Ultrasonic Cleaner, SONICA[®], Soltec, Milan, Italy).

Dynamic light scattering (DLS) measurements were performed on a W130i instrument (Avid Nano, High Wycombe, UK), at 20 °C, to analyze the mean particle size and the PI of NM by using a quartz cell (Hellma[®] Analytics, 111-QS, 10 mm × 10 mm, Jena, Germany). The hydrodynamic particle size was calculated by the cumulant method. The surface charge of NM was recorded by measuring the zeta potential (ZP) in a Zetasizer Nano ZS equipment (Malvern Instruments Inc., Malvern, UK) at 20 °C. All the measurements were performed in triplicate.

The determination of copper, zinc and titanium concentrations released from NM into different culture media was performed by inductively coupled plasma optical emission spectrometry (ICP-OES) (Horiba Jobin Yvon, Activa M, Longjumeu, France). The suspensions were prepared at 20 mg L⁻¹ according to the procedure described above,

centrifuged at 6000 rpm for 30 min, followed by the acidification of the supernatant with HNO_3 1% (v/v).

2.3. Maintenance of Organism Cultures and Human Cell Lines

Freshwater green microalgae *R. subcapitata* were maintained in our laboratory and cultivated in 4-L glass flasks containing sterile medium (Woods Hole MBL) [25] in a growth chamber under continuous light, at 20 ± 2 °C, 6000–10,000 Lux (cool white light fluorescent lamps), with constant aeration.

L. minor plants were originally collected from the Botanic Garden (University of Porto) and the best fitted plants were washed with distilled water and maintained in an Erlenmeyer containing Steinberg growth medium [26] under 16 h^L:8 h^D, at 20 ± 2 °C and light intensity of 6000–10,000 Lux, provided by cool white light fluorescent lamps. The culture medium was renewed once a week.

Adult crustaceans *D. magna* were cultured in the glass flasks (~30 animals/800 mL) containing ASTM hard water [27] supplemented with organic extract, vitamins and suspension of green microalgae *R. subcapitata* provided for food. The medium was replaced three times per week and the animals were maintained at a constant temperature (20 ± 2 °C) with a natural light–dark cycle.

The human cell lines Caco-2 (derived from human colorectal adenocarcinoma), SV-80 (human lung fibroblast) and HaCaT (human keratinocytes) were purchased from Cell Line Services (CLS; Eppelheim, Germany) and HepG2 (human hepatic carcinoma; American Type Culture Collection (ATCC) N° HB-8065TM) were kindly offered by Prof. Carlos Palmeira from Coimbra University, Portugal. Cells were cultured in DMEM containing FBS (10%, v/v), penicillin (100 U mL⁻¹), streptomycin (100 µg mL⁻¹) and 1 mM L-glutamine. All cell cultures were maintained in an incubator at 37 °C under a humidified atmosphere of 5% CO₂. The culture medium was replaced every 2 days.

2.4. Ecotoxicity Assays

2.4.1. *R. Subcapitata* Growth Inhibition Test

The microalgae growth inhibition tests were performed according to OCDE 201 protocol [28]. The stock culture was previously prepared by adding 20 mL of algae inoculum to 50 mL of MBL medium and incubated under 16^L:8^D, at 21 ± 2 °C, during 72 h. After this period, the density of algae in the original stock suspension was determined through optical microscopy on the Neubauer chamber, diluted in MBL, to obtain an initial density of 10⁴ cells mL⁻¹, and seeded in 24-well microplates.

For the toxicity assay, NM were dispersed into MBL medium (please see Section 2.3). The tested concentrations ranged from 0 to 20 mg L⁻¹ (dilution factor of 1.6) for nano-CuO, hydrophilic nano-TiO₂, hydrophilic nano-SiO₂ and SiO₂ (30% aq. suspension). For nano-ZnO, the tested concentrations ranged from 0 to 5 mg L⁻¹ (dilution factor of 1.4). For the assay, each concentration was tested in triplicate, while the control group was tested in sextuplicate. The microplates were maintained under the same conditions as described above for the culture and homogenized manually twice a day with a micropipette to avoid algal agglomerates. The cell density in each replica was counted through an optical microscope using a Neubauer chamber. The microalgae growth inhibition (in percentage) for each concentration of NM was determined in relation to the control group (without NM).

2.4.2. *L. Minor* Growth Inhibition Test

L. minor growth test was based on the OECD guideline 221 [26]. Three colonies with three fronds each were transferred to test vessels containing a volume of 60 mL (only Steinberg medium for the control group or Steinberg medium plus NM for the treatment groups) under axenic conditions. For each test vessel, the number of colonies and the frond number were the same. Plants were exposed to suspensions of NM at concentrations ranging from 0 to 20 mg L⁻¹ with a dilution factor of 1.6, except for nano-CuO, in which the tested concentrations ranged from 0 to 1.9 mg L⁻¹, also applying a dilution factor

of 1.6. Regarding nano-CuO, we initially tested a concentration range of 0 to 20 mg L⁻¹. However, a severe decrease in *L. minor* growth rate was observed with concentrations above 1.9 mg L⁻¹.

The toxicity test for each concentration and control group was performed in triplicate and maintained in the same conditions as described for the stock culture maintenance. Three colonies with tree fronds were collected from the stock culture plants and dried at 60 °C overnight to provide the initial dry weight of the plants. The effect of NM was evaluated according to the growth rate of *L. minor* calculated based on the number of fronds and on the dry weight of the fronds after 7 days of exposure.

2.4.3. *D. Magna* Immobilization Test

Acute toxicity test using *D. magna* was performed according to OECD guideline 202 [29]. The toxicity test was assessed using five *D. magna* neonates (age < 24 h) per glass tube (i.e., per replicate) containing 25 mL ASTM hard water medium with different concentrations of the NM in suspension. Nano-TiO₂, hydrophilic nano-SiO₂, nano-SiO₂ (30% aq. suspension) were tested at concentrations ranging from 0 to 20 mg L⁻¹ (dilution factor of 1.6). Nano-CuO was tested at concentrations ranging from 0 to 7.3 (dilution factor of 1.4), while nano-ZnO was tested from 0 to 1.9 mg L⁻¹ (dilution factor of 1.6). Each concentration was tested in quadruplicate. The tubes were incubated under the same conditions as described above for the culture maintenance. After 24 h and 48 h of exposure to suspensions of NM, the immobilization of the organisms was visually inspected, and the number of immobilized organisms was counted, taking into account their ability to swim freely within 15 s.

2.5. Cytotoxicity Tests with Human Cell Lines

The assessment of NM cytotoxicity was performed using the AlamarBlue® (AB) reagent as an indicator of cell proliferation and viability [30]. Viable cells are able to reduce AB (resazurin, blue color) to resorufin (pink color) and therefore the oxidation/reduction reaction can be quantitatively measured by reading the absorbance of culture media. Cell's viability correlates with the percentage of AB reduction, which can be determined as previously reported in Andreani et al. (2014) [30].

For the procedure, cells were detached using a trypsin-EDTA solution at 37 °C for 7 min, counted using an automated cell counter (TC10—, BIORAD, Amadora, Portugal) and diluted in culture medium (with FBS) to adjust the cellular density to 5 × 10⁴ cell mL⁻¹. Then, cells were seeded in 96-well plates (100 µL/well) and cultured for 24 h to allow cell attachment. After this, the culture medium was removed and replaced by FBS-free culture medium containing the dispersions of NM at final concentrations of 0.0, 5.0, 10, 15 and 20 mg L⁻¹ and incubated for 24 or 48 h, at 37 °C and 5% CO₂ atmosphere. The toxicity of each concentration was evaluated in quadruplicate and cells not exposed to NM were used as negative controls. Subsequent to the incubation time (24 or 48 h), the culture media of the control group and of the treatment groups were removed and AB solution (10% (v/v) prepared in fresh FBS-free culture medium) was added to each well (100 µL/well), followed by an additional incubation for 4 h (controlled humidity, 37 °C and 5% CO₂). Then, a Labsystem Multiskan EX microplate reader (LabX, Midland, ON, Canada) was used to read the absorbance of each well at 570 and 620 nm. As stated by Doktorovová et al. (2014), a biologically inert NM is one that elicits a cell viability equal to or higher than 70% [31].

2.6. Statistical Analysis

For all experiments, the data were reported as mean ± standard deviation (SD). Statistically significant differences between treatments for each assay and parameter assessed were tested by univariate analysis of variance (ANOVA) with subsequent Dunnett's post hoc test to determine the differences between each treatment and the control group. No observed effect concentrations (NOEC) and low observed effect concentrations (LOEC) were

determined based on the previously described analysis. The EC50 and EC20 values were determined by applying non-linear least squares regression analysis using STATISTICA® 7.0 software (StatSoft, Inc., Tulsa, OK, USA). For *D. magna* immobilization assay, lethal concentrations (LC₅₀) were estimated after fitting a Probit regression to the binary data [32] using SPSS® Statistics software version 25 (Chicago, IL, USA).

In order to provide predicted no-effect concentrations (PNEC) or hazard concentrations for 5% of the species (HC₅) for the NM under evaluation and for the freshwater organisms, deterministic and probabilistic approaches were followed by applying assessment factors or by obtaining species sensitivity distributions (SSD), respectively [33,34]. For the estimation of PNEC and HC₅ values, data from the literature were selected (Table S1) when they were reported for the same NM tested in this study, regarding its chemical nature, independently of the particle size reported by the manufacturer. The SSD were generated only for two NM, for which EC₅₀ values were available (LOEC and NOEC values were not used, since they are not statistical estimations), for 6 different species by fitting a linearized log-normal model to data, with the USEPA SSD Generator V1 (USEPA, Boston, MA, USA), available at <https://www.epa.gov/caddis-vol4/caddis-volume-4-data-analysis-download-software>. When more than one data point was available for the same species and endpoint, a geometric mean was calculated. For PNEC or HC₅ estimation, a bibliographic search was carried out in May 2020 by using the ISI WEB of Science database and by combining the following keywords: TS = (nano*) AND TS = (titanium dioxide) AND TS = (toxicity or Ecotoxic*) AND TS = (freshwater). The search was repeated for silicon dioxide, silica dioxide, zinc oxide and copper oxide. All the papers found were analyzed and it was decided to use only those that tested the toxicity of NM following standard guidelines for ecotoxicological assays with freshwater species.

3. Results and Discussion

3.1. Behavior of NM in Culture Media

The behavior and physical characterization of NM suspended in the different culture/test media were investigated by DLS and electrophoretic mobility. The characterization of NM in regard to hydrodynamic particle size, PI and ZP is depicted in Table 1. Data from physicochemical parameters clearly showed the formation of particle agglomerates. Strong agglomeration was observed especially for dispersions of nano-CuO in ASTM, Steinberg and DMEM test media, for nano-TiO₂ in ASTM and DMEM media and for nano-ZnO in Steinberg medium, achieving average hydrodynamic sizes out of the range of the equipment measurements. In opposition, nano-SiO₂ (aq) dispersed in MBL or ASTM was revealed to have a particle size closer to that supplied by the manufacturer (~10 nm), with a homogenous size distribution, as shown by the low PI values. From the ZP measurements, all NM presented negative surface charges when suspended in the different culture media. The low surface charge (absolute values) of NM correlates directly with the drastic increase in the average hydrodynamic size of NM, suggesting the high instability of the suspensions. For all NM, the absolute highest ZP values were observed when NM were dispersed into MBL (>|20 mV|), showing that these dispersions may present moderate stability compared to the others. However, as can be observed from the data, although the hydrophilic nano-SiO₂ dispersed into MBL showed a high PI (0.86), the ZP value is also high. The same occurred with nano-SiO₂ (aq) when dispersed in ASTM, showing a decrease in ZP values in comparison with MBL suspensions (from −27.3 to −15.3 mV), despite the decrease in the PI value. Therefore, although NM dispersions with |ZP| > 30 mV are considered stable, ZP measurements only refer to the electrostatic effect (repulsive forces) between particles but do not supply any information on the attractive van der Waals forces, which may also play a role in nanoparticle stability. According to the well-known classic theory of Derjaguin, Landau, Verwey and Overbeek (DLVO), the particle stabilization can be explained as a superposition of the repulsive electrostatic potential and the attractive van der Waals forces [35]. Thus, in high-ionic-strength environments, the particle agglomeration

can be attributed to a decrease in repulsive forces due to a compression of the electrical double layer and an increase in van der Waals interactions [36].

Table 1. Average hydrodynamic size \pm standard deviation (SD), polydispersity index (PI), average zeta potential (ZP \pm SD) and concentration of the free metal ions recorded in the nanomaterials (NM) dispersions prepared in different culture media at 20 mg L⁻¹.

NM	Culture Medium	Hydrodynamic Particle Size (nm \pm SD)	PI	ZP (mV \pm SD)	Free Metal Ions (mg L ⁻¹)
Nano-CuO	MBL	223.3 \pm 76.3	0.34	-22.8 \pm 2.9	<0.05
	ASTM	>1 μ m	0.76	-5.9 \pm 0.3	0.9
	Steinberg	>1 μ m	-*	-7.9 \pm 1.1	8.5
	DMEM without FBS	>1 μ m	-*	-2.3 \pm 0.7	4.3
Nano-TiO ₂	MBL	770.5 \pm 174.8	0.92	-21.6 \pm 0.8	0.15
	ASTM	>1 μ m	-*	-9.4 \pm 2.7	0.65
	Steinberg	899.7 \pm 75.9	0.92	-9.9 \pm 0.4	3.9
	DMEM without FBS	>1 μ m	-*	-4.3 \pm 0.7	0.14
Hydrophilic nano-SiO ₂	MBL	209.2 \pm 180.0	0.86	-27.3 \pm 3.8	-
	ASTM	235.2 \pm 104.2	0.44	-15.3 \pm 1.0	-
	Steinberg	195.5 \pm 85.6	0.43	-8.4 \pm 1.8	-
	DMEM without FBS	162.9 \pm 147.6	0.90	-21.3 \pm 1.4	-
Nano-SiO ₂ (aq)	MBL	11.8 \pm 2.6	0.22	-25.7 \pm 2.0	-
	ASTM	12.5 \pm 1.6	0.13	-13.9 \pm 1.3	-
	Steinberg	50.0 \pm 26.0	0.52	-9.8 \pm 0.6	-
	DMEM without FBS	119.6 \pm 57.0	0.47	-10.8 \pm 6.4	-
Nano-ZnO	MBL	178.6 \pm 116.6	0.65	-27.5 \pm 1.1	0.7
	ASTM	281.8 \pm 214.8	0.76	-2.2 \pm 0.1	3.4
	Steinberg	>1 μ m	-*	-10.2 \pm 1.2	5.1
	DMEM without FBS	300.1 \pm 195.2	0.65	-6.7 \pm 0.1	1.7

Note: * Indicates that DLS measurements were not able to calculate the PI values, since the cumulant method is not suitable for the highly polydispersed formulations.

As reported by several works, the particle size can be affected by environmental pH, ionic strength and by the presence of plasma proteins [37,38]. Although there are numerous types of NM, various homogenization techniques (sonication, magnetic stirring or vortex) and homogenization times, our results were consistent with others reported in the literature. As described above, in the present study, nano-TiO₂ (stabilized with HNO₃, anatase phase) showed severe particle agglomeration when dispersed in the different culture media after sonication in a water bath. In accordance with our results (Table 1), Nogueira et al. (2015) also showed high particle agglomeration (high Z-Ave and PI) concomitantly with a low ZP after the suspension of nano-TiO₂ (anatase phase) in ASTM, MBL and Steinberg media through magnetic stirring [18], suggesting that sonication does not bring great benefits in terms of NM suspension stability. In addition, these authors also reported that nano-TiO₂ in MBL showed lower particle agglomeration and higher ZP values when compared with the dispersion of nano-TiO₂ in ASTM or Steinberg media. Although nano-TiO₂ type P25 (combination of anatase and rutile phases) is different from the nano-TiO₂ tested in this study (anatase), a study conducted by Ji et al. (2010) also reported that nano-TiO₂ type P25 suspended in DMEM by sonication (in a water bath) and by vortex showed high particle agglomeration, obtaining a hydrodynamic diameter of 843 nm, a PI of 0.021 and a ZP of -7.4 mV [36]. In this study (Table 1), DMEM was in fact the media causing the highest particle agglomeration for almost all the tested NM. Contrarily to our data (Table 1), the agglomeration of particles observed by Ji et al. (2010) was not accompanied by an increase in PI value, indicating that even in the agglomeration state, the size of the particles remains homogeneous.

The concentration of free ions in the test medium is an important parameter that may affect the toxic behavior of metallic NM [39]. According to the free ion quantification, a direct connection between the free metal ions in the culture media and the particle agglomeration was observed for all NM dispersions (Table 1). Results indicate that, for all tested NM, the highest concentrations of dissolved metal ions in the culture media were also detected when high particle agglomeration was recorded. In addition, the highest concentrations of soluble metal ions were found in Steinberg medium, for all NM, while the lowest concentrations were detected in MBL for nano-CuO and nano-ZnO and in DMEM for nano-TiO₂ (Table 1). Although there was a direct correlation between high particle agglomeration and high concentration of free metal ions, this result can be likely ascribed to the pH of the different culture media used in the present study. The low pH of Steinberg medium (around 5.5) may contribute to the higher release of metal ions compared with the other media, since the pH levels in MBL and ASTM are around 7.2 and 8.0, respectively. In addition, although high particle agglomeration was observed, it is possible that there were small particles contributing to the increase in free metal ion concentration. This hypothesis is supported by the high PI values recorded, which point towards polydisperse suspensions.

3.2. Effect of NM on *R. Subcapitata* Growth

After 72 h of exposure, nano-CuO induced high toxicity to algae *R. subcapitata*, with an EC₅₀ of 12.77 mg L⁻¹ (Figure 1A). Nevertheless, nano-ZnO was the most toxic NM to *R. subcapitata*, depicting an EC₅₀ = 4.86 mg L⁻¹ (Figure 1B, Table 2). The growth curves demonstrated that, for nano-TiO₂, a significant difference in the algae growth rate compared with the control group was only observed at 20 mg L⁻¹ ($p < 0.05$), where the growth inhibition was 27% (Figure 1C). Similar results were obtained for hydrophilic nano-SiO₂ and nano-SiO₂ (aq), for which the percentage of algae growth inhibition at 20 mg L⁻¹ was 30% and 23.9%, respectively (Figure 1D,E). In addition, a slight growth stimulation ($p < 0.05$) was observed for nano-SiO₂ (aq) at the lowest tested concentration (1.9 mg L⁻¹). In general, there is consensus in the scientific community about the effect of NM size on organisms. Our results suggest that for the algal growth inhibition assay, there was no obvious relationship between the particle size and toxicity. For example, nano-CuO and nano-ZnO showed high particle agglomeration when suspended in MBL (Table 1) and induced high toxicity to *R. subcapitata*. However, nano-TiO₂ showed low toxicity to microalgae despite agglomeration, while nano-SiO₂ (aq), for which a smaller particle average size was recorded, did not display toxic effects to *R. subcapitata* up to 12.5 mg L⁻¹.

Table 2. Effective concentrations (EC₂₀ and EC₅₀ values), LOEC and NOEC of NM obtained for microalgae growth inhibition and (EC₅₀) for *D. magna* immobilization after 24 and 48 h of exposure.

NM	EC ₂₀ and EC ₅₀ Values for Algae Growth Inhibition (mg L ⁻¹)				EC ₅₀ Values for <i>D. magna</i> Immobilization (mg L ⁻¹)	
	EC ₂₀	EC ₅₀	LOEC	NOEC	24 h	48 h
Nano-CuO	3.08 (1.24–4.92)	12.77 (8.84–16.70)	3.1	1.9	5.00 (4.27–6.20)	1.78 (0.21–2.66)
Nano-ZnO	4.11 (4.00–4.21)	4.86 (4.81–4.91)	3.6	2.5	11.88 (ND)	1.33 (ND)
Nano-TiO ₂	>20	>20	20	12.5	>20	>20
Nano-SiO ₂	>20	>20	7.8	4.9	>20	>20
Nano-SiO ₂ (aq)	>20	>20	1.9	-	>20	>20

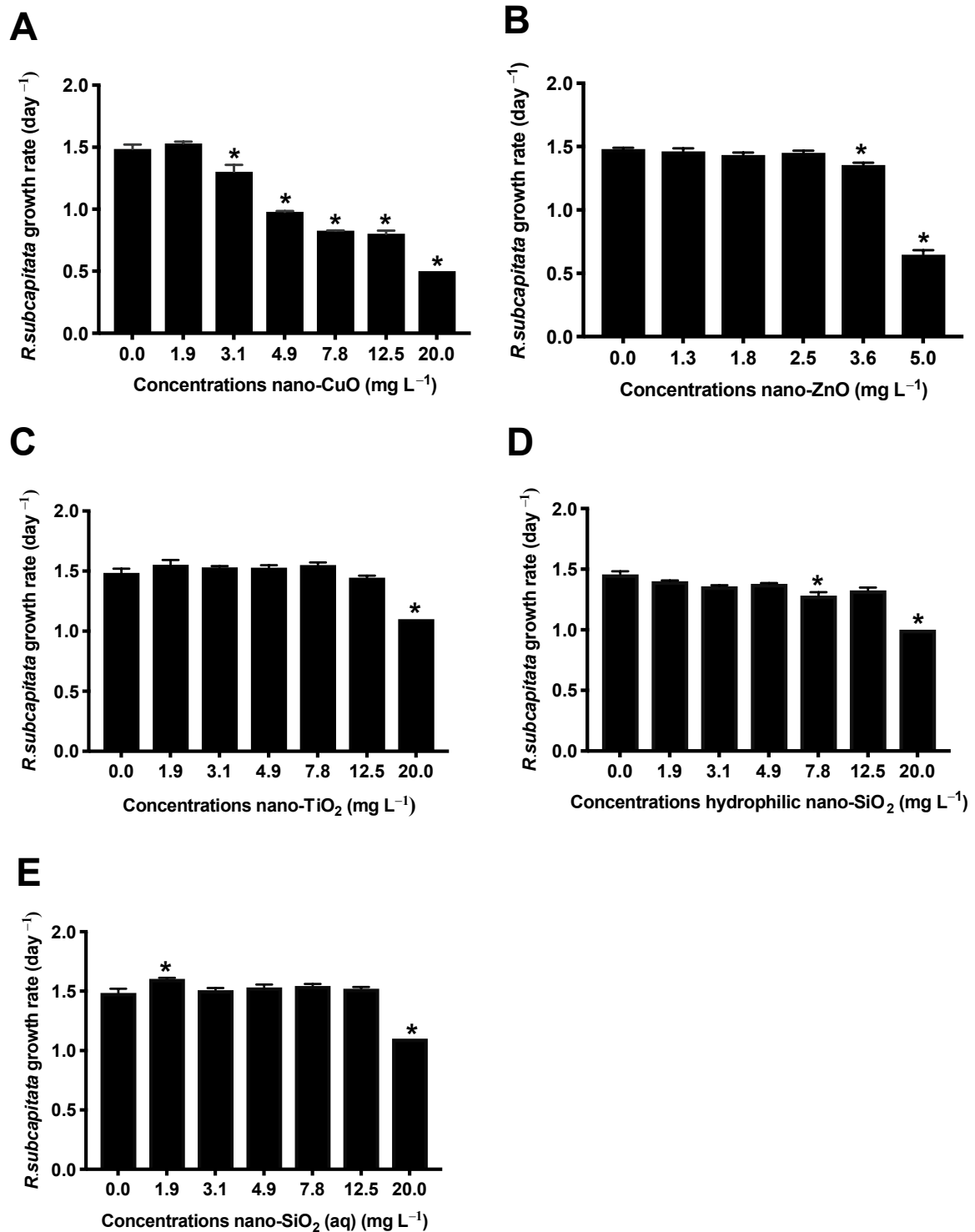


Figure 1. *R. subcapitata* growth rate after 72 h of exposure to nano-CuO (A), nano-ZnO (B), nano-TiO₂ (C), hydrophilic nano-SiO₂ (D), nano-SiO₂ (aq) (E). The experiments were conducted in triplicate and the results are shown as the mean ± standard deviation (ANOVA followed by Dunnett's test, * $p < 0.05$ compared to control).

It is well known that the toxicity of nano-CuO to organisms has been associated with the particles themselves [40] and/or the release of metal ions from NM [41]. In the present work, the amount of Cu^{+2} ions released from nano-CuO was very low ($<0.05 \text{ mg L}^{-1}$) and, thus, the observed toxicity may be explained by other mechanisms related to nano-CuO per se. In this context, due to the dark color of the nano-CuO suspensions and their high particle agglomeration in MBL, the attachment of nano-CuO onto the algal surface could have led to the physical shading effect, reducing the availability of light, as reported for other dark NM [42]. However, this effect alone is not enough to explain the nano-CuO toxicity to algae. The strong effect of nano-CuO on *R. subcapitata* could have been caused by the direct physical contact with algal cells followed by NM internalization, leading to deleterious effects, such as plasma membrane and cellular organelle damage. As suggested by Melegari et al. (2013), after the attachment of nano-CuO onto the algal surface, lipid peroxidation may occur, giving rise to new pores in the membrane which may contribute to nano-CuO internalization [40]. Once internalized, nano-CuO can be intracellularly transformed in nano- Cu_2O , which is a chemical entity that releases Cu^{+2} [43], inducing high toxic effects by generating reactive oxygen species (ROS) [44]. Although the pore size of the cell wall of algae ranges from 5 to 20 nm, the size of these pores can be increased in the reproductive phase and even the interaction between the NM and algae can lead to the generation of larger pores [45]. However, in fact, all of these studies demonstrate that the mechanisms of NM interaction with cells are diverse, and all may play their role in NM toxicity.

Our results are in agreement with some studies showing that, in general, nano-ZnO is much more toxic than other metal oxide NM [46]. Although there are many studies focusing on the toxicity mechanisms of nano-ZnO on microalgae, the mechanism of toxicity of these NM remains unclear. A great deal of experimental evidence has suggested that the toxicity of nano-ZnO is mainly driven by the release of Zn^{+2} from NM [41], while other studies have shown that the release of Zn^{+2} cannot explain, by itself, the high toxicity of nano-ZnO [47]. In the present study, the nano-ZnO suspension in MBL contained nano-ZnO agglomerates and dissolved Zn^{+2} ions (Table 1). Therefore, these two factors may have contributed to inhibiting the growth of microalgae. However, it was observed that 72-h EC_{50} for nano-ZnO (4.86 mg L^{-1}) was higher than the Zn^{+2} concentration dissolved in MBL (0.7 mg L^{-1}), which suggests that the toxicity of nano-ZnO was not driven only by the dissolved ions. Even in an agglomeration state, nano-ZnO was able to cause severe toxicity to algae at low concentrations. Aravantinou et al. (2017) also suggested that nano-ZnO in large aggregates can be deposited on the algal surface, leading to toxic effects [48]. In this case, it is highly probable that the nano-ZnO toxicity mechanism can be similar to the one described above for nano-CuO. Inside the cells, nano-ZnO may suffer from dissolution into Zn^{+2} , leading to the toxicity on microalgae, as demonstrated by other studies [49,50].

As described above, in our study, anatase nano- TiO_2 showed low toxicity to *R. subcapitata*, as algae growth only decreased at 20 mg L^{-1} ($p < 0.05$). Since we tested anatase nano- TiO_2 functionalized with HNO_3 , we hypothesize that this functionalization decreased the production of ROS by nano- TiO_2 or reduced the direct interaction between NM and the microalgae cellular wall. Generally, nano- TiO_2 anatase has been demonstrated to be more toxic than nano- TiO_2 rutile since this type of crystal structure is more chemically reactive, resulting in an increase in ROS generation [51]. Nevertheless, Nogueira et al. (2015) also observed that anatase nano- TiO_2 (non-functionalized) stimulated *R. subcapitata* growth at concentrations of 16 and 20 mg L^{-1} and at a high agglomeration state (average particle size: $1225 \pm 26 \text{ nm}$) [18].

From the obtained results, both nano- SiO_2 showed no toxicity to algae at all the tested concentrations, except for the highest (20 mg L^{-1}). Hydrophilic nano- SiO_2 , which is a fumed NM, presented higher particle agglomeration in algae culture medium, while nano- SiO_2 (30% aq. suspension), colloidal NM, showed low particle agglomeration. It is well known that the fumed nano- SiO_2 has greater ability to produce hydroxyl radicals in comparison to colloidal nano- SiO_2 , then inducing higher toxic effects. However, if we

examine our data, the type of nano-SiO₂, as well as the particle size, were not relevant to the toxicity results, since both formulations showed similar behavior regarding their effect on *R. subcapitata*. Our data are in agreement with other studies, even testing other forms of this NM, which reported 72-h EC₂₀ values of 20 ± 5 and 28.8 ± 3.2 mg L⁻¹ in *R. subcapitata* for commercial colloidal silica LUDOX[®] with hydrodynamic size of 12.5 and 27 nm, respectively [52]. Yu et al. (2018) also observed a 96-h EC₅₀ = 1180.725 mg L⁻¹ for commercial nano-SiO₂ even in the agglomeration state (hydrodynamic size of 570.27 ± 27.83 nm in TAP (Tris-Acetate Phosphate medium) in *Chlamydomonas reinhardtii* [53].

3.3. Growth Inhibition Effect of NM on *L. Minor*

The effects of NM on *L. minor* growth assessed by frond number and dry weight after 7 days of exposure are represented in Figure 2. Nano-CuO was the most toxic NM to *L. minor* among the other tested NM, followed by nano-ZnO. As shown in Figure 2A, after 7-day exposure, the dry weight of the plants was not significantly influenced when compared with the unexposed group. However, the number of *L. minor* fronds was drastically decreased, by 41.17%, after nano-CuO exposure at 1.9 mg L⁻¹. The Cu²⁺ ions can inhibit photosystem II activities [54] and cause oxidative stress in different aquatic species, as reported by previous studies [55,56]. Yue et al. (2018) attributed the significant reduction of 32 and 33% in frond number and dry weight, respectively, in *L. minor* exposed to 0.15 mg L⁻¹ of commercial nano-CuO, for 7 days, to the internalization of nano-CuO (or the Cu²⁺ ions released from NM) by roots, followed by the generation of ROS, mainly H₂O₂ and OH radical species [57]. On the contrary, Shi et al. (2011) observed that nano-CuO synthesized in the laboratory, per se, showed higher toxicity to the aquatic plant *Landoltia punctata* in comparison to the free Cu ions, after exposure to 1.0 mg L⁻¹ nano-CuO for 9 days, which inhibited 50% of plant growth [58]. In this case, the synthesis of nano-CuO may have involved other compounds or left impurities responsible for the highest toxicity when compared to the commercial NM. Nano-ZnO (Figure 2B) was also toxic to *L. minor*, decreasing significantly the plant growth regarding both frond number and dry weight of fronds at all the tested concentrations in comparison to the control group. In the present study, DLS measurements showed the high particle agglomeration of both NM (nano-CuO and nano-ZnO) after their dispersion in Steinberg medium. In addition, the highest concentration of the dissolved ions, from both NM, was observed in *L. minor* medium. Therefore, soluble Cu²⁺ and Zn²⁺ ions may have been responsible, at least in part, for the toxic effects detected in *L. minor*, as previously described for the microalgae *R. subcapitata* (Figure 1). As shown in other reports, free zinc ions were absorbed by plants and contributed to the toxicity of commercial nano-ZnO to *Spirodela polyrhiza* L. at 50 mg L⁻¹ [59]. Chen et al. (2016) also attributed the toxicity of commercial nano-ZnO to *L. minor* to the dissolved Zn ions in the medium at 10 mg L⁻¹ of ZnO and at low pH [60].

For nano-TiO₂ stabilized by HNO₃, no growth inhibition was detected when *L. minor* plants were exposed even at the highest tested concentrations (Figure 2C). In fact, there was a slight stimulation at the highest concentrations regarding the frond number ($p < 0.05$). Nogueira et al. (2015) found no toxicity of nano-TiO₂ anatase (non-functionalized) for *L. minor* at concentrations up to 20 mg L⁻¹ after 7 days of exposure [18]. These results confirm once again that functionalization with HNO₃ did not enhance the toxicity of nano-TiO₂.

According to the obtained results, both nano-SiO₂ suspensions were not toxic to *L. minor* at the tested concentrations (Figure 2D,E). To the best of our knowledge, there are no studies regarding the toxicity of nano-SiO₂ to *Lemna* species. In fact, although Si is not an essential element for plant growth, Si can be accumulated by aquatic plants, leading to several beneficial effects, such as resistance and protection against pathogens and metals' toxicity [61].

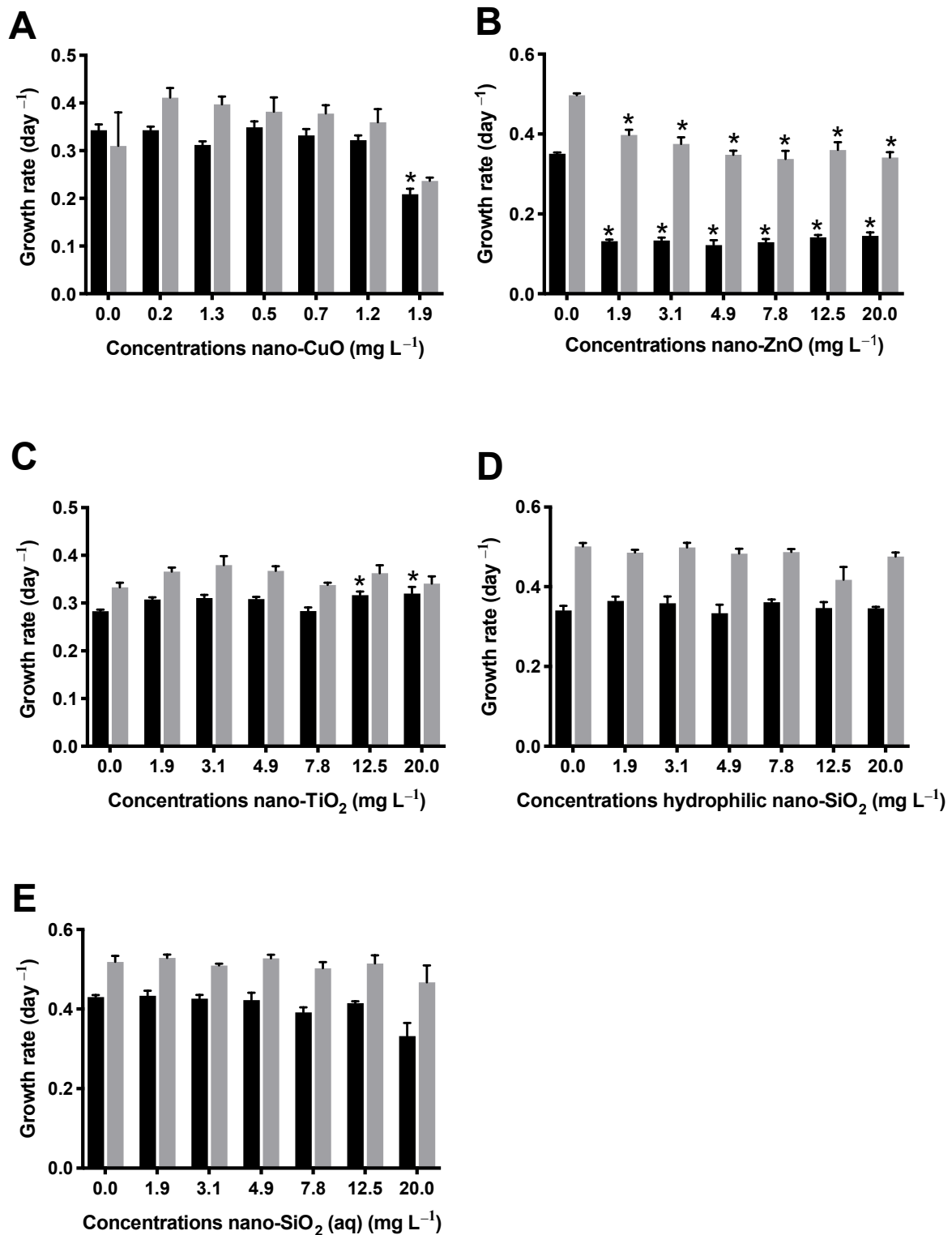


Figure 2. Average growth rate (day⁻¹) regarding the frond number (black bars) and dry weight of fronds (grey bars) of *L. minor* exposed to the different concentrations of nano-CuO (A), nano-ZnO (B), nano-TiO₂ (C), hydrophilic nano-SiO₂ (D), nano-SiO₂ (aq) (E) for 7 days. The experiments were conducted in triplicate and the results are shown as the mean ± standard deviation (ANOVA followed by Dunnett's test, * $p < 0.05$ compared to control).

3.4. Acute Effects of NM on *D. Magna*

The acute toxicity to *D. magna* was recorded after 24 and 48 h of exposure. *D. magna* survival was dramatically affected by both nano-CuO and nano-ZnO, showing a 48 h-EC₅₀ of 1.78 mg L⁻¹ for nano-CuO and 1.33 mg L⁻¹ for nano-ZnO (Figure 3 and Table 2).

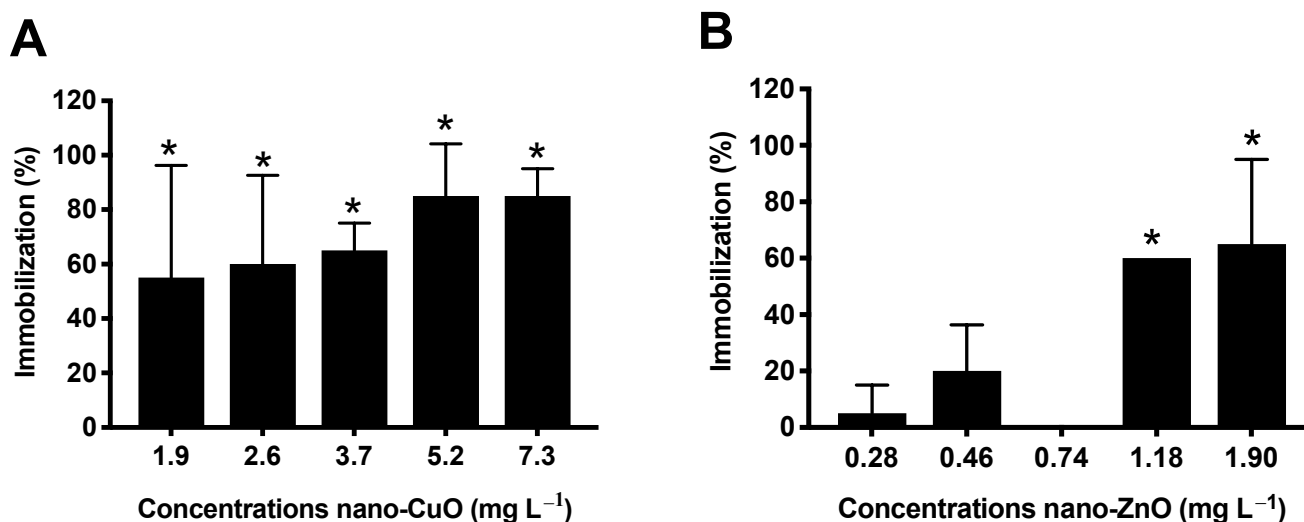


Figure 3. Percentage of *D. magna* immobilization exposed to nano-CuO (A) and nano-ZnO (B) suspensions for 48 h. Values are reported as the mean of four replicates \pm standard deviation (ANOVA followed by Dunnett's test, * $p < 0.05$ compared to control). Along the toxicity assays, the neonatal immobilization percentage in the control group was 0%.

Nano-CuO displayed a dose-dependent response in *D. magna*, with only 15% of organisms with activity at the maximum tested concentration (7.3 mg L⁻¹), after 48 h of exposure (Figure 3A). Nano-ZnO was shown to be even more toxic, since at the maximum concentration tested (1.9 mg L⁻¹), only 35% of organisms with activity were recorded after 48 h of exposure (Figure 3B). As observed in the microalgae growth inhibition test, the toxicity of NM was not related with their particle size. As shown in Table 1, even in a high particle agglomeration state, nano-ZnO and nano-CuO induced high toxicity to the cladocerans, while nano-TiO₂ and hydrophilic nano-SiO₂ (both with high particle agglomeration) and SiO₂ (aq) (particle size of 12.51 nm in ASTM) did not affect this filter feeding organism. Regarding the toxicity of nano-CuO on *D. magna*, it has been attributed to the presence of Cu ions in the medium. However, in our study, the concentration of dissolved ions in ASTM was 0.9 mg L⁻¹ for nano-CuO (Table 1), and due to this low concentration of dissolved ions, it is highly probable that the toxicity of nano-CuO is not driven by Cu ions only. Considering that daphnids are filter feeding organisms, NM aggregates may have exerted their effect through gut clogging or through physical interaction with antennae.

Concerning nano-ZnO toxicity, the concentration of Zn ions in ASTM was of 3.4 mg L⁻¹, and therefore, the toxicity of nano-ZnO to neonates can be related, at least in part, to the presence of Zn ions dissolved in the medium, as was also suggested by other studies testing commercial nano-ZnO in *D. magna* at concentrations ranging from 0.08 to 8 mg L⁻¹ [62]. In addition, it is well known that *D. magna* are able to ingest and accumulate NM smaller than 50 μ m [63]. Therefore, in this context, we believe that both nano-CuO and nano-ZnO could have been filtered and ingested by the daphnids, as reported by Xiao et al. (2015) [64]. These authors estimated a LC₅₀ of 0.99 mg L⁻¹ (nano-ZnO) and 0.093 mg L⁻¹ (nano-CuO) for *D. magna* and concluded that, at concentrations of nano-CuO and nano-ZnO above 0.1 mg L⁻¹ and 1.0 mg L⁻¹, respectively, the particles exerted a significant effect on daphnids compared to their soluble salts due to the ingestion and adhesion effect of NM to daphnids carapace.

As seen in Table 2, the results revealed no toxicity of nano-TiO₂ and nano-SiO₂ (aq) to *D. magna*, resulting in 100% of active organisms even at 20 mg L⁻¹. As described previously, nano-TiO₂ anatase tested in this study was stabilized by HNO₃, and there are no other data regarding the toxicity of this NM stabilized by HNO₃. However, other studies testing the acute toxicity of nano-TiO₂ anatase to daphnids indicate that this stabilization may have contributed to reducing the toxicity of these NM. For example, Novak et al. (2018) obtained an NOEC of 1 mg L⁻¹ and LOEC of 10 mg L⁻¹ (lower than that obtained in our study) after 48-h exposure of *D. magna* to nano-TiO₂ in anatase form without the presence of stabilizer agents (primary particle of 5 nm and hydrodynamic size in ISO water of 375 nm) [65].

3.5. Critical Analysis of Available Ecotoxicological Data for Risk Assessment Purposes

As shown in Table S1 in the Supplementary Materials, which only presents published studies that followed standard protocols to test the toxicity of the NM (ISO or OECD guidelines), it is evident that different works tested different forms of the same NM (different physicochemical properties, surface modifications, functionalization of NM), the number of test species is limited, the characterization of the NM is frequently performed in a water suspension and not in the test media, and all these aspects contribute to the lack of useful data for the derivation of environmental threshold levels, by probabilistic methods—for example, through the application of species sensitivity distributions [66]. This is unfortunately true for all the NM under evaluation in this study, despite being apparently the most studied NM—for example, nano-TiO₂. Regarding nano-CuO, a direct comparison of acute toxicity to *D. magna* was only possible between our study and the studies of Adam et al. (2015) [67], Kim et al. (2017) [68] and Muna et al. (2019) [69], for NM primary sizes between 20 and 50 nm (Table S1). EC₅₀ values for *D. magna* acute immobilization tests were 12 times higher [70] than those found in our studies, probably due to the use of a different test medium. The same occurred when the data reported by Aruoja et al. 2009 [41], for *L. minor* growth inhibition, are compared with ours. Once again, and despite the same test protocol being followed, the used test media were different, and the primary size of particles reported by these authors is smaller than that reported in our study. No toxicity endpoints for other test species can be obtained from the literature for nano-CuO, except for *H. incongruens* [69], if we consider the above range of NM sizes, rather than looking to a specific particle size. This may be considered acceptable if we take into account that it is difficult to expose organisms to NM at the particle size reported by the manufacturer, since particle agglomeration frequently occurs in the test media. Table 3 displays the toxicity endpoints that were used for the estimation of a PNEC value for nano-CuO. Values expressed in concentration of Cu were converted to concentration of CuO. Whenever available, only chronic endpoints were taken into account and an assessment factor of 10 was used, considering that three endpoints for three species from different trophic levels were available. The PNEC value obtained is 2.65 times higher than that obtained by Chen et al. (2018) (0.049 mg L⁻¹) [33], which is in part unexpected, since the assessment factors are usually a more conservative approach. Nevertheless, it is not clear which data were actually used by these authors.

Table 3. Predicted no-effect concentrations (PNEC) or hazard concentrations for 5% of the species (HC₅) and corresponding 95% confidence intervals, estimated for the NM under evaluation in this study.

	Species	Endpoint	mg L ⁻¹		
Nano-CuO					
Primary particle average size (20–50 nm)	<i>R. subcapitata</i>	72 h-EC ₅₀ (growth inhibition)	12.8	This study	
	<i>H. incongruens</i>	6d-EC ₅₀ (mortality)	2.4	[69]	
	<i>D. magna</i>	Average number of neonates	1.3	[67]	
	PNEC (AF = 10)		0.13		
Nano-ZnO					
Primary particle average size (<100 nm)	<i>R. subcapitata</i>	72 h-EC ₅₀ (growth inhibition)	4.86	This study	
	<i>D. magna</i>	EC ₅₀ (immobilization)	1.3	This study	
			1.9	[69]	
			3.1	[71]	
			1.4	[68]	
	<i>H. incongruens</i>	Geometric mean 6d-EC ₅₀ (mortality)		0.37	[69]
		<i>D. pulex</i>	48 h-EC ₅₀ (immobilization)	0.24	[72]
		<i>S. rubescens</i>	28d-IC ₅₀ (Growth rate)	8.93	[48]
	<i>T. platyurus</i>	6d-EC ₅₀ mortality	0.22	[73]	
	HC ₅ r ² = 0.898		0.063 (95%CI:0.01–0.35)		
Nano-TiO₂ anatase stabilized with HNO₃					
Primary particle average size (4–8 nm)—anatase	<i>R. subcapitata</i>	72 h-EC ₅₀ (growth inhibition)	20.0	This study	
	PNEC (AF = 100)		0.2		
Nano-TiO₂ anatase					
Primary particle average (<25 nm)—anatase	<i>C. reinhardtii</i>	96 h-EC ₅₀ Growth rate	359.8	[53]	
	<i>S. obliquus</i>	72 h-EC ₅₀ (growth rate)	136.9	[74]	
	<i>Scenedesmus sp.</i>	72 h-EC ₅₀ (growth rate)	21.2	[75]	
	<i>Chlorella sp.</i>	72 h-EC ₅₀ (growth rate)	16.12	[75]	
	<i>C. dubia</i>	48 h-LC ₅₀ immobilization	37.04	[76]	
	<i>R. subcapitata</i>	72 h-EC ₅₀ Growth rate	2.7	[77]	
	HC ₅ r ² = 0.977		1.89 (95% CI: 0.83–4.31)		
Nano-SiO₂ hydrophilic					
Primary particle average size (<25 nm)	<i>R. subcapitata</i>	72 h-EC ₅₀ Growth rate	7.8	This study	
	PNEC (AF = 100)		0.08		

Table 3. Cont.

	Species	Endpoint	mg L ⁻¹	
Nano-SiO ₂ (aqueous)	<i>R. subcapitata</i>	72 h-EC ₅₀ Growth rate	1.9	This study
Primary particle average size (10 nm)		PNEC (AF = 100)	0.02	
Nano-SiO ₂				
Primary particle average size (10–20 nm)	<i>C. reinhardtii</i>	72 h-EC ₅₀ Growth rate	1180.7	[53]
		PNEC (AF = 100)	11.8	

Note: LOECs and NOECs were not used for PNEC and HC₅ estimations.

For nano-ZnO, more toxicity data are available compared with the other NM (Table S2), some of which helped to confirm the sensitivity of *D. magna*, since they provided EC₅₀ values of the same order of magnitude, if we consider particle sizes > 100 nm. The exception is the study of Zhu et al. (2009), which showed a level of sensitivity two-times lower than that recorded in our study, for a NM with a similar primary size [78]. Further, some additional species were tested, including, for example, *H. incongruens*, *D. pulex*, *S. rubens* and *T. platyurus* [48,69,72,73]. For these NM, it was possible to generate an SSD as data for six different species (Figure 4A). However, to overcome the lack of data, it was necessary to combine the data from acute and chronic tests and for a range of primary sizes, as shown in Table 3. The HC₅ recorded was once again three-times greater than that proposed by Chen et al. (2018). However, as mentioned above, it is not clear which data were used by these authors to generate HC₅ [33].

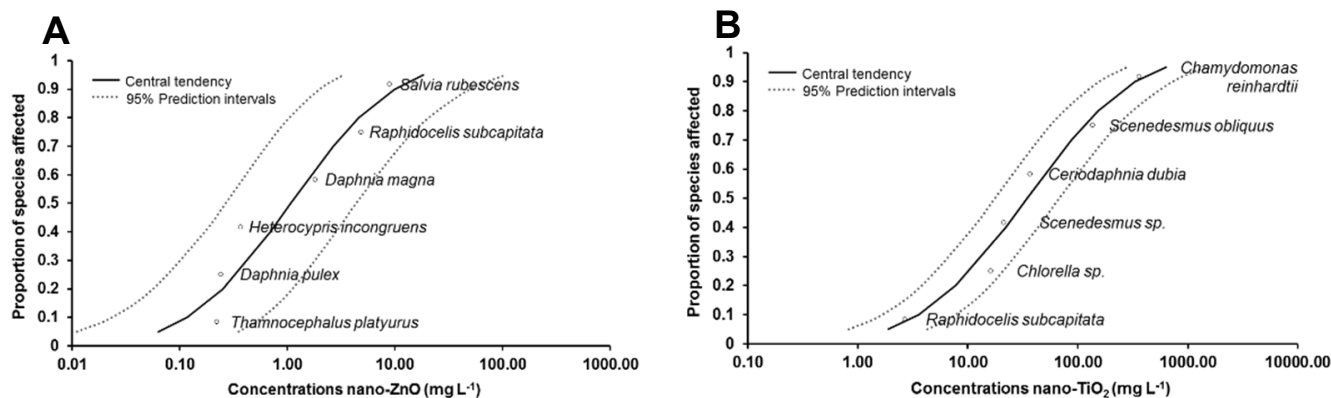


Figure 4. Species sensitivity distribution curves obtained by fitting toxicity endpoints to linearized log-normal model to toxicity endpoints available for nano-ZnO (A) and nano-TiO₂ (B).

Regarding nano-TiO₂ (Table S3), considered the most studied metal oxide NM, the diversity of the NM tested is in fact very high, making it difficult to obtain sufficient data for the derivation of HC₅ values for each one, using probabilistic methodologies. However, it is clear that our study is the only one providing toxicity data for hydrophilic TiO₂ stabilized by HNO₃. The data selected allowed us to estimate an HC₅ for TiO₂ anatase of 1.89 mg L⁻¹ (primary particle size < 25 nm, anatase), which was different from those proposed by Chen et al. (2018) [33] (Figure 4B). In our study, we provided a threshold only for anatase nano-TiO₂. However, we have combined acute and chronic endpoints, since otherwise, the available data were even fewer. Chen et al. (2018) did not take into account the difference in the mineral nature of this NM. Regarding the NM tested in our study (nano-TiO₂ stabilized with HNO₃, anatase), only one endpoint was used to estimate a PNEC value, thus providing an extremely protective value, which points towards the higher risk of this NM when compared with their non-stabilized form. This value is not in

agreement with the lowest toxicity suggested for this NM and by the LOEC and NOEC values recorded. The same occurred for nano-SiO₂ (Table S4), which is the less studied NM, with very few data available supported by standard protocols and thus useful for risk assessment purposes. The lack of data available gave rise to two PNEC values, for the silica-based NM tested in this study, which are also extremely protective considering that almost all the ecotoxicological data point towards the low toxicity of these NM.

3.6. Cytotoxicity of NM to Human Cell Lines

Since *in vitro* cytotoxicity studies may elucidate the mechanisms of toxicity and evaluate the acute toxicity of the compounds, in this study, Caco-2, HepG2, HaCaT and SV-80 cell lines were used to assess the impact of NM exposure on humans, through different pathways. Figure 5 shows the cell viability data for the different cell lines incubated with NM, for 48 h, at concentrations ranging from 2 to 20 mg L⁻¹. According to the results, nano-CuO was the most toxic NM to intestine and liver cells (Figure 5A,B). Nano-CuO caused a significant reduction in Caco-2 cell viability (~40–50%) at concentrations ≥ 10 mg L⁻¹ after 48 h of exposure (Figure 5A). For HepG2 cells, nano-CuO was able to induce higher toxicity even at the lowest tested concentration (2 mg L⁻¹), reaching a plateau (cell viability around 45%; Figure 5B). However, these NM showed low toxicity to the lung and skin cell lines (Figure 5C,D). There are very few studies that investigate the effect of nano-CuO on human cell lines and how nano-CuO could induce cytotoxicity is still unclear. Previous studies have demonstrated that the release of Cu⁺² ions from nano-CuO may be responsible for the high toxicity of these NM [79]. Therefore, since, in our study, nano-CuO exhibited some solubility in the cell culture medium (4.3 mg L⁻¹), it is possible that free Cu ions also contributed to the nano-CuO effects. In the same way, Piret et al. (2012) showed that at 25 mg L⁻¹, spherical and rod-shaped commercial nano-CuO (average size of 50 and 12 nm) decreased Caco-2 cell viability in 20 and 30%, respectively, after 48 h of exposure. These authors also attributed the observed toxicity to the release of Cu⁺² and to the shape of NM [80]. The same authors reported a decrease in HepG2 cell viability after exposure to commercial nano-CuO at concentrations of 20–80 mg L⁻¹ of Cu, attributing this effect to the production of ROS [81]. As described above, nano-CuO did not induce any toxic effect on HaCaT cells (Figure 5D), maintaining the cell viability above 70% when compared to the control group. Similar results were obtained by Luo et al. (2014), who reported low toxicity of synthesized nano-CuO (5–7 nm) in HaCaT human keratinocytes at 20 mg L⁻¹ after 24 h of exposure [82].

Regarding the effects of nano-CuO on SV-80 cells, a decrease of 20% in cell viability at 20 mg L⁻¹ was observed. There are no studies regarding the toxicity of nano-CuO on the SV-80 cell line. However, for comparison, other studies have reported a decrease in the viability of human lung epithelial cells (A549 cell line) in ~90 and 93% after 18 h of exposure to 40 and 80 mg L⁻¹ of commercial nano-CuO (hydrodynamic particle size of 220 nm), respectively [83].

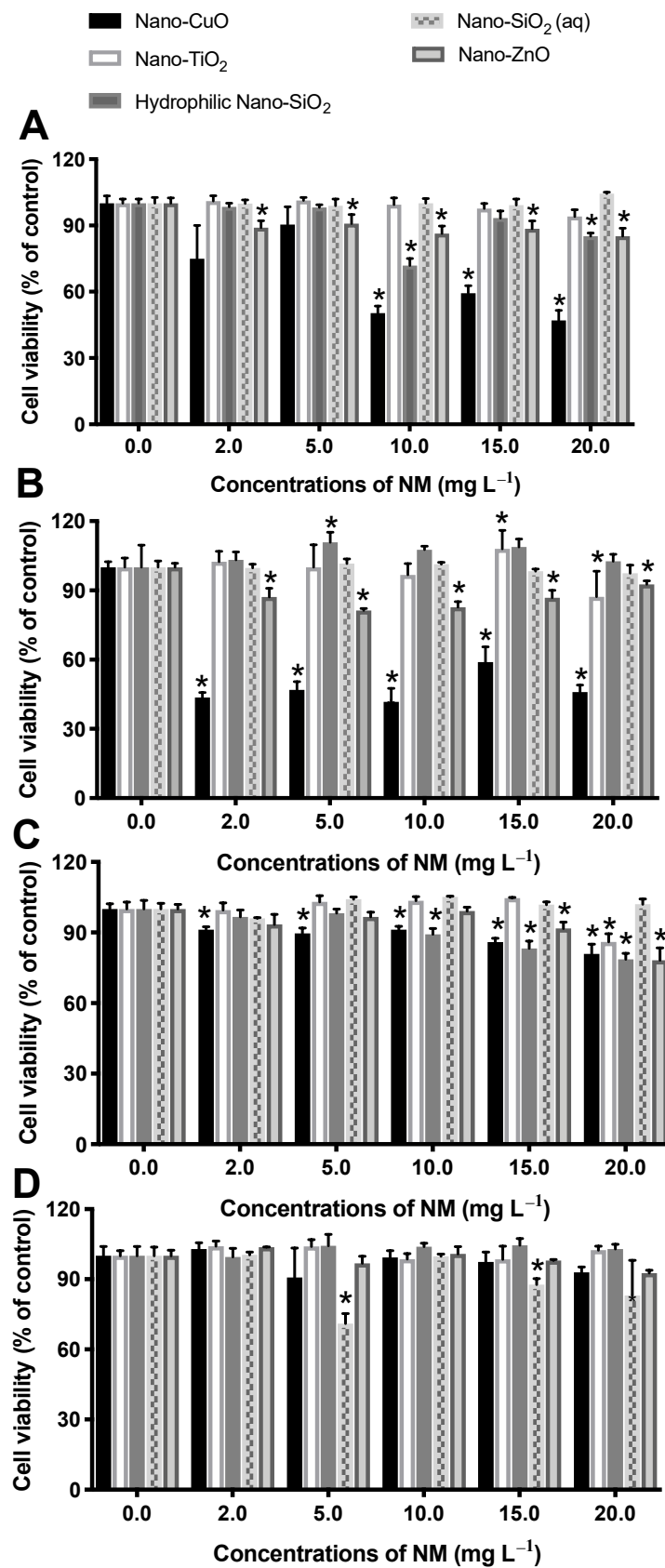


Figure 5. Cell viability of Caco-2 (A), HepG2 (B), SV-80 (C) and HaCaT (D) cells, after 48 h exposure to different NMs, as denoted, at concentrations ranging from 2 to 20 mg L⁻¹. Results are expressed as the percentage of control, and for each cell line, each concentration was tested in quadruplicate. Control group corresponds to non-exposed cells, set as 100% of cell viability. Significant differences in cell viability compared to the control group are indicated by * $p < 0.05$ (ANOVA followed by Dunnett's test).

In the present study, nano-ZnO was shown to be biocompatible for all selected human cell lines at the tested concentrations. The decrease in cell viability was more pronounced for SV-80 cells (21.8%) after exposure to nano-ZnO at 20 mg L⁻¹. The data regarding the in vitro toxicity of nano-ZnO to human cells are very controversial. Abbot et al. (2013) only detect high toxicity (50% reduction in cell viability) for commercial nano-ZnO (hydrodynamic particle size 212–260 nm) to Caco-2 cells, after 48 h of exposure at 100 mg L⁻¹ [84]. However, Abbasi-Oshaghi et al. (2016) demonstrated a significant decrease in Caco-2 cell viability (40%) at 20 mg L⁻¹, after 24 h of exposure to synthesized nano-ZnO in the laboratory (20–30 nm measured by TEM) [85]. Sharma et al. (2012) also showed that exposure to 14–20 mg L⁻¹ of commercial nano-ZnO (hydrodynamic particle size of 267 nm) for 12 h reduced the HepG2 cells' viability and induced cell death by apoptosis [86]. As seen in Figure 5, nano-ZnO also did not induce any toxic effects on human keratinocyte cells (HaCaT). Vinardell et al. (2017) showed an IC₅₀ of 50 mg L⁻¹ after 48 h of HaCaT cells' exposure to commercial nano-ZnO with 100 nm [87], which is in agreement with our study that reports no toxicity at concentrations up to 20 mg L⁻¹. Lee et al. (2012) also observed a low effect of commercial nano-ZnO at 20 mg L⁻¹ (decrease in HaCaT cell viability of 25% compared with the control cells) after 24 h of exposure [88]. The in vitro cell toxicity of nano-ZnO is generally attributed to the release of Zn⁺² from nanoparticles [89] as well as to the induction of cellular oxidative stress due to the generation of ROS [89–91]. However, the toxicity mechanisms of nano-ZnO are not clearly established. A study performed by Chen et al. (2019) showed that at concentrations above 16 mg L⁻¹, the toxicity of commercial nano-ZnO (hydrodynamic particle size 37–200 nm) to HepG2 cells was ascribed to the release of Zn⁺² after 24 h of exposure [16]. However, in our study, the concentration of Zn ions in DMEM was very low (1.7 mg L⁻¹) and, therefore, it is possible that the absence of toxicity can be attributed to the low concentration of soluble ions in the cell culture medium.

From our study, nano-TiO₂ anatase was not toxic to any of the cell lines at the tested concentrations, which is in agreement with the previously reported data. As demonstrated by several works, data for the cytotoxicity of nano-TiO₂ are consistent despite the various types of TiO₂ NM tested (different crystalline structures, particle size, surface charge), cell culture medium used, time of exposure and methods followed to evaluate the cell viability.

Commercial nano-TiO₂, even in the particle agglomeration state (hydrodynamic particle size of 212–260 nm in Caco-2 cell medium), was not toxic to Caco-2 cells at concentrations ranging from 0.1 to 100 mg L⁻¹ after 48 h of exposure [84]. Tada-Oikawa et al. (2016) observed no toxicity to Caco-2 cells after 24-h exposure to commercial nano-TiO₂ with different crystal structures (anatase and rutile) and particle sizes (primary particle sizes of 50 and 100 nm; hydrodynamic particle sizes of 227.78 and 253.4 nm in DMEM containing serum) [92]. Wang et al. (2011) also did not observe toxic effects for nano-TiO₂ (crystal structure not reported; particle size of 17–64 nm provided by TEM) in HepG2 cells after 48-h exposure at concentrations ranging from 25 to 200 mg L⁻¹ [93]. Rutile nano-TiO₂ (hydrodynamic particle size of 447.2 nm in HepG2 serum-free medium) was not toxic to Caco-2 cells at concentrations up to 25 mg L⁻¹, after 24 h of exposure [94]. In fact, some studies postulate that the presence of serum in the cell culture medium can lead to a reduction in particle agglomeration [95]. In our study, the cytotoxicity assays were conducted in FBS-free DMEM, resulting in high particle agglomeration. Nevertheless, given all the information available, and despite the nano-TiO₂ tested in our study to be different from the other studies, since it was stabilized with HNO₃, the results conclusively point towards the biocompatibility of these NM.

No sign of severe toxic effects, in all tested cell lines, was observed for both nano-SiO₂ suspensions in DMEM after 48 h of incubation. However, as described previously for the other NM, there are several types of nano-SiO₂ (crystalline, amorphous, mesoporous) synthesized and tested by different methodologies and exposure time, respectively, which in turn make it difficult to compare their toxicological effects [96]. In our study, we tested the commercial fumed amorphous nano-SiO₂ with hydrophilic properties (probably due to a surface functionalization which was not specified by the manufacturer; hydrodynamic

particle size of 162.86 nm in DMEM) and the commercial colloidal amorphous nano-SiO₂ in aqueous suspensions (hydrodynamic particle size of 119.56 nm in DMEM) after 48 h of exposure through the AlamarBlue (AB) method. In opposition to our results, Ahmad et al. (2012) showed that commercial amorphous nano-SiO₂ (hydrodynamic particle size of 96 nm in cell culture medium) at concentrations up to 10 mg L⁻¹ did not decrease significantly HepG2 cell viability measured by MTT and neutral red uptake (NRU) methods and for a longer time period of exposure (72 h) [97]. Using commercial amorphous nano-SiO₂ (primary particle size of 15 nm) and the MTT cell viability method, for a shorter period of time (24 h), Gong et al. (2017) observed a decrease of almost 50% in HaCaT cell viability at 20 mg L⁻¹ [98], which was the highest concentration tested in our study (Figure 5D). Contrarily, Liang et al. (2014) observed no toxicity for HaCaT cells when exposed to nano-SiO₂ (particle size of 50 nm measured by TEM) synthesized by the Stöber method at 25 mg L⁻¹ after 4 h of exposure [99]. Regarding HepG2 and Caco-2 cells, Andreani et al. (2014) also evaluate the cytotoxicity of synthesized colloidal amorphous nano-SiO₂ (lyophilized using trehalose 10% (w/v, 1:1) as cryoprotectant; hydrodynamic particle size of 290 nm measured in ultrapure water) by the Stöber sol-gel method and observed no toxicity for Caco-2 and HepG2 cells at concentrations of 0–500 mg L⁻¹ after 48 h of exposure measured by AB assay [30]. Different cytotoxicity results have been obtained by Li et al. (2011), who compared four types of synthesized colloidal nano-SiO₂ with different sizes (hydrodynamic particle sizes of 628.5, 127.3, 108.8 and 82.2 nm measured in DMEM after 24 h) and demonstrated size-dependent cytotoxicity of nano-SiO₂. However, only nano-SiO₂ with smaller particle size decreased the viability of HepG2 cells (the cell viability was determined by the WST-8 cell counting kit (CCK-8)) in ~20 and 30% at a concentration of 12.5 and 25 mg L⁻¹, respectively, after 24 h of exposure. The other nano-SiO₂ did not significantly reduce the cell viability at concentrations up to 100 mg L⁻¹ [100].

As described above, cytotoxicity data regarding the metal oxide NM (commercial or lab synthesized) may differ depending on the type of NM, cells involved, toxicological assays and incubation time. Gastrointestinal and respiratory tracts, as well as the skin, are the organs that can be widely exposed to the toxic effects of these entities and, therefore, more research and the harmonization of experimental processes by standard protocols are urgently needed to guarantee the safe application of NM [101]. In addition, the lack of consideration of a NM characteristics–toxicity relationship in most toxicological studies can lead to uncertain or erroneous conclusions [101].

4. Conclusions

In the present study, the effect of different metal oxide NM, namely nano-CuO, nano-TiO₂, nano-SiO₂ and nano-ZnO, on three aquatic freshwater species (*R. subcapitata*, *D. magna* and *L. minor*) and on human cell lines (Caco-2, HepG2, SV-80 and HaCaT) has been evaluated. From the data obtained in this study, most of the NM showed the tendency to agglomerate after their dispersion into the different culture media used for the maintenance of distinct test species. However, the particle agglomeration did not prevent the NM from exerting their toxic effects. Nano-CuO and nano-ZnO, despite the particle agglomeration, were consistently toxic to freshwater organisms, *R. subcapitata*, *D. magna* and *L. minor*, at the tested concentrations. The opposite results were recorded for nano-TiO₂ (high particle agglomeration state) and nano-SiO₂ (low particle agglomeration for nano-SiO₂ (aq) and high particle agglomeration for hydrophilic nano-SiO₂), in which no toxicity was observed for the tested aquatic species.

Concerning the NM effect on human cell lines, results showed that the viability of SV-80 and HaCaT cells was little affected by NM after 48-h incubation, with the cell viability remaining 70% higher than the control. However, nano-CuO was very toxic to Caco-2 and HepG2 cells, especially at the highest tested concentrations, while nano-TiO₂, nano-SiO₂ and ZnO were not cytotoxic to the different human cell lines. No relationship was found between NM particle size and cytotoxicity for the tested NM. The toxicity can be related to

the adsorption of NM to biological membranes or to the generation of ROS, but also to the presence of the ions in the cell medium, mainly for nano-CuO and nano-ZnO suspensions.

An extensive bibliographic search and compilation of data available in the literature demonstrated that data for the ecotoxicity and cytotoxicity of NM, even for those NM apparently more tested, are still very scarce, since most of the published studies were performed using different forms of NM. The risk thresholds estimated (HC₅ and PNEC values) are still highly protective, since they are based on few toxicity data. However, this study provides consistent evidence of the potential risks of both nano-CuO and nano-ZnO to aquatic organisms and also their effect on public health.

Although great effort has been made by OECD and ISO to adapt the standard protocols to the specificities of nanomaterials, there are no new standard protocols to replace those used in this study or in the previous studies reviewed in this manuscript. For example, for aquatic tests, OECD published in 2020 a guidance document on the aquatic and sediment toxicological testing of nanomaterials (Guidance Document 317) that is not intended to replace existing protocols but to adapt the existing Test Guidelines for reliable NM testing. Therefore, the harmonization of experimental processes by standard protocols and follow-up of OECD guidelines already published, such as OECD 318 (2017), must be considered and respected in order to guarantee data quality as well as their application in risk assessment evaluation.

Supplementary Materials: The following are available online at <https://www.mdpi.com/2079-4991/11/1/66/s1>, Table S1: Physicochemical characteristics and toxic effects of different nano-CuO on freshwater species. The primary particle size was supported by the manufacturer. NR: data not reported; Table S2: Physicochemical characteristics and toxic effects of different nano-ZnO on freshwater species. The primary particle size was supported by the manufacturer. NR: data not reported; Table S3: Physicochemical characteristics and toxic effects of different nano-TiO₂ on freshwater species. The primary particle size was supported by the manufacturer. NR: data not reported; Table S4: Physicochemical characteristics and toxic effects of different nano-SiO₂ on freshwater species. The primary particle size was supported by the manufacturer. NR: data not reported.

Author Contributions: Conceptualization and experimental design: T.A., C.M.P. and R.P.; Methodology, data treatment and scientific discussion: T.A., C.M.P., R.P., V.N., S.F., J.L.R., V.V.P., A.G., M.J.F. and A.M.S.; resources: C.M.P., A.M.S., M.J.F. and R.P.; writing—original draft preparation: T.A.; writing—review and editing: R.P., C.M.P. and A.M.S.; supervision: R.P. and C.M.P.; project administration and funding acquisition: T.A., C.M.P., M.J.F. and R.P. All authors have read and agreed to the published version of the manuscript.

Funding: This work was partially supported by national funds through the Fundação para Ciência e Tecnologia (FCT) under the scope of the project SaFe NPest (POCI-01-0145-FEDER-029343) (P2020/CO MPETE) and by the project NANOFOOT—Materials, Components and Footwear with enhanced comfort properties based on nanotechnologies (Grant Agreement No. 606570-FP7-SME- 2013 Research for the Benefit of SMEs). This research was also supported by the Foundation of Science and Technology through the Strategic Funding UIDB/00081/2020. The authors also acknowledge the contribution from the Strategic Funding of GreenUPorto (IUIDB/05748/2020).

Institutional Review Board Statement: Not applicable.

Informed Consent Statement: Not applicable.

Data Availability Statement: All data have been illustrated in the manuscript.

Conflicts of Interest: The authors declare no conflict of interest.

References

1. Hanus, M.J.; Harris, A.T. Nanotechnology innovations for the construction industry. *Prog. Mater. Sci.* **2013**, *58*, 1056–1102. [[CrossRef](#)]
2. Mitrano, D.M.; Motellier, S.; Clavaguera, S.; Nowack, B. Review of nanomaterial aging and transformations through the life cycle of nano-enhanced products. *Environ. Int.* **2015**, *77*, 132–147. [[CrossRef](#)] [[PubMed](#)]

3. Bressot, C.; Manier, N.; Pagnoux, C.; Aguerre-Chariol, O.; Morgeneyer, M. Environmental release of engineered nanomaterials from commercial tiles under standardized abrasion conditions. *J. Hazard. Mater.* **2017**, *322*, 276–283. [[CrossRef](#)] [[PubMed](#)]
4. Kaegi, R.; Sinnet, B.; Zuleeg, S.; Hagedorfer, H.; Mueller, E.; Vonbank, R.; Boller, M.; Burkhardt, M. Release of silver nanoparticles from outdoor facades. *Environ. Pollut.* **2010**, *158*, 2900–2905. [[CrossRef](#)]
5. Potter, P.M.; Navratilova, J.; Rogers, K.R.; Al-Abed, S.R. Transformation of silver nanoparticle consumer products during simulated usage and disposal. *Environ. Sci. Nano* **2019**, *6*, 592–598. [[CrossRef](#)]
6. Gagnon, V.; Button, M.; Boparai, H.K.; Nearing, M.; O'Carroll, D.M.; Weber, K.P. Influence of realistic wearing on the morphology and release of silver nanomaterials from textiles. *Environ. Sci. Nano* **2019**, *6*, 411–424. [[CrossRef](#)]
7. Geranio, L.; Heuberger, M.; Nowack, B. The behavior of silver nanotextiles during washing. *Environ. Sci. Technol.* **2009**, *43*, 8113–8118. [[CrossRef](#)]
8. Kittler, S.; Greulich, C.; Diendorf, J.; Köller, M.; Epple, M. Toxicity of silver nanoparticles increases during storage because of slow dissolution under release of silver ions. *Chem. Mater.* **2010**, *22*, 4548–4554. [[CrossRef](#)]
9. Parks, A.N.; Cantwell, M.G.; Katz, D.R.; Cashman, M.A.; Luxton, T.P.; Ho, K.T.; Burgess, R.M. Assessing the release of copper from nanocopper-treated and conventional copper-treated lumber into marine waters I: Concentrations and rates. *Environ. Toxicol. Chem.* **2018**, *37*, 1956–1968. [[CrossRef](#)]
10. Surette, M.C.; Nason, J.A. Nanoparticle aggregation in a freshwater river: The role of engineered surface coatings. *Environ. Sci. Nano* **2019**, *6*, 540–553. [[CrossRef](#)]
11. Li, L.; Liu, T.; Fu, C.; Tan, L.; Meng, X.; Liu, H. Biodistribution, excretion, and toxicity of mesoporous silica nanoparticles after oral administration depend on their shape. *Nanomedicine* **2015**, *11*, 1915–1924. [[CrossRef](#)] [[PubMed](#)]
12. Recordati, C.; De Maglie, M.; Bianchessi, S.; Argenti, S.; Cella, C.; Mattiello, S.; Cubadda, F.; Aureli, F.; D'Amato, M.; Raggi, A.; et al. Tissue distribution and acute toxicity of silver after single intravenous administration in mice: Nano-specific and size-dependent effects. *Part. Fibre Toxicol.* **2016**, *13*, 12. [[CrossRef](#)] [[PubMed](#)]
13. Groh, K.J.; Dalkvist, T.; Piccapietra, F.; Behra, R.; Suter, M.J.-F.; Schirmer, K. Critical influence of chloride ions on silver ion-mediated acute toxicity of silver nanoparticles to zebrafish embryos. *Nanotoxicology* **2015**, *9*, 81–91. [[CrossRef](#)] [[PubMed](#)]
14. Dominguez, G.A.; Lohse, S.E.; Torelli, M.D.; Murphy, C.J.; Hamers, R.J.; Orr, G.; Clapper, R.D. Effects of charge and surface ligand properties of nanoparticles on oxidative stress and gene expression within the gut of *Daphnia magna*. *Aquat. Toxicol.* **2015**, *162*, 1–9. [[CrossRef](#)]
15. Manzo, S.; Miglietta, M.L.; Rametta, G.; Buono, S.; Di Francia, G. Toxic effects of ZnO nanoparticles towards marine algae *Dunaliella tertiolecta*. *Sci. Total Environ.* **2013**, *445*, 371–376. [[CrossRef](#)]
16. Chen, P.; Wang, H.; He, M.; Chen, B.; Yang, B.; Hu, B. Size-dependent cytotoxicity study of ZnO nanoparticles in HepG2 cells. *Ecotoxicol. Environ. Saf.* **2019**, *171*, 337–3346. [[CrossRef](#)]
17. Andreani, T.; Nogueira, V.; Pinto, V.; Ferreira, M.; Rasteiro, M.; Silva, A.; Pereira, R.; Pereira, C.M. Influence of the stabilizers on the toxicity of metallic nanomaterials in aquatic organisms and human cell lines. *Sci. Total Environ.* **2017**, *607–608*, 1264–1277. [[CrossRef](#)]
18. Nogueira, V.; Lopes, I.; Rocha-Santos, T.A.P.; Rasteiro, M.G.; Abrantes, N.; Gonçalves, F.; Soares, A.M.V.M.; Duarte, A.C.; Pereira, R. Assessing the ecotoxicity of metal nano-oxides with potential for wastewater treatment. *Environ. Sci. Pollut. Res.* **2015**, *22*, 13212–13224. [[CrossRef](#)]
19. Neale, P.A.; Jämting, Å.K.; O'Malley, E.; Herrmann, J.; Escher, B.I. Behaviour of titanium dioxide and zinc oxide nanoparticles in the presence of wastewater-derived organic matter and implications for algal toxicity. *Environ. Sci. Nano* **2015**, *2*, 86–93. [[CrossRef](#)]
20. Song, L.; Connolly, M.; Fernández-Cruz, M.L.; Vijver, M.G.; Fernández, M.; Conde, E.; de Snoo, G.R.; Peijnenburg, W.J.G.M.; Navas, J.M. Species-specific toxicity of copper nanoparticles among mammalian and piscine cell lines. *Nanotoxicology* **2014**, *8*, 383–393. [[CrossRef](#)]
21. Newman, M.D.; Stotland, M.; Ellis, J.I. The safety of nanosized particles in titanium dioxide- and zinc oxide-based sunscreens. *J. Am. Acad. Dermatol.* **2009**, *61*, 685–692. [[CrossRef](#)] [[PubMed](#)]
22. D'Agata, A.; Fasulo, S.; Dallas, L.J.; Fisher, A.S.; Maisano, M.; Readman, J.W.; Jha, A.N. Enhanced toxicity of “bulk” titanium dioxide compared to “fresh” and “aged” nano-TiO₂ in marine mussels (*Mytilus galloprovincialis*). *Nanotoxicology* **2014**, *8*, 549–558. [[CrossRef](#)] [[PubMed](#)]
23. Chang, H.; Jwo, C.S.; Lo, C.H.; Tsung, T.T.; Kao, M.J.; Lin, H.M. Rheology of CuO nanoparticle suspension prepared by ASNSS. *Rev. Adv. Mater. Sci.* **2005**, *10*, 128–132.
24. Heroult, J.; Nischwitz, V.; Bartczak, D.; Goenaga-Infante, H. The potential of asymmetric flow field-flow fractionation hyphenated to multiple detectors for the quantification and size estimation of silica nanoparticles in a food matrix. *Anal. Bioanal. Chem.* **2014**, *406*, 3919–3927. [[CrossRef](#)]
25. Nichols, H.W. Growth media-freshwater. In *Handbook of Phycological Methods*; Cambridge University Press: Cambridge, UK, 1973; pp. 16–17.
26. OECD. *Guidelines for the Testing of Chemicals. Lemna sp. Growth Inhibition Test No. 206*; Organisation for Economic Co-Operation and Development: Paris, France, 2004.
27. ASTM. *Standard Practice for Conducting Acute Toxicity Test with Fishes, Macroinvertebrates and Amphibians*; Report E-729-80; American Standards for Testing and Materials: Philadelphia, PA, USA, 1980.

28. OECD. *Guidelines for Testing of Chemicals. Freshwater Algae and Cyanobacteria, Growth Inhibition Test No. 201*; Organisation for Economic Co-Operation and Development: Paris, France, 2006.
29. OECD. *Guidelines for Testing of Chemicals. Daphnia sp., Acute Immobilization Test No. 202*; Organisation for Economic Co-Operation and Development: Paris, France, 2004.
30. Andreani, T.; Kiill, C.P.; Souza, A.L.R.; Fangueiro, J.F.; Fernandes, L.; Doktorovová, S.; Santos, D.L.; García, M.L.; Gremião, M.P.D.; Souto, E.B.; et al. Surface engineering of silica nanoparticles for oral insulin delivery: Characterization and cell toxicity studies. *Colloids Surf. B* **2014**, *123*, 916–923. [[CrossRef](#)]
31. Doktorovova, S.; Souto, E.B.; Silva, A.M. Nanotoxicology applied to solid lipid nanoparticles and nanostructured lipid carriers—A systematic review of in vitro data? *Eur. J. Pharm. Biopharm.* **2014**, *87*, 1–18. [[CrossRef](#)]
32. Finney, D.J. *Probit Analysis*, 3rd ed.; Cambridge University Press: Cambridge, UK, 1971.
33. Chen, G.; Peijnenburg, W.J.G.M.; Xiao, Y.; Vijver, M.G. Developing species sensitivity distributions for metallic nanomaterials considering the characteristics of nanomaterials, experimental conditions, and different types of endpoints. *Food Chem. Toxicol.* **2018**, *112*, 563–570. [[CrossRef](#)]
34. European Commission. *Technical Guidance Document on Risk Assessment No 1488/94*; European Commission Joint Research Centre: Ispra, VA, Italy, 2003.
35. Missana, T.; Adell, A. On the applicability of DLVO theory to the prediction of clay colloids stability. *J. Colloid Interface Sci.* **2000**, *230*, 150–156. [[CrossRef](#)]
36. Ji, Z.; Jin, X.; George, S.; Xia, T.; Meng, H.; Wang, X.; Suarez, E.; Zhang, H.; Hoek, E.M.V.; Godwin, H.; et al. Dispersion and stability optimization of TiO₂ nanoparticles in cell culture media. *Environ. Sci. Technol.* **2010**, *44*, 7309–7314. [[CrossRef](#)]
37. Jiang, J.; Oberdörster, G.; Biswas, P. Characterization of size, surface charge, and agglomeration state of nanoparticle dispersions for toxicological studies. *J. Nanoparticle Res.* **2009**, *11*, 77–89. [[CrossRef](#)]
38. Lynch, I.; Salvati, A.; Dawson, K.A. What does the cell see? *Nat. Nanotechnol.* **2009**, *4*, 546. [[CrossRef](#)] [[PubMed](#)]
39. Song, L.; Vijver, M.G.; Peijnenburg, W.J.G.M. Comparative toxicity of copper nanoparticles across three Lemnaceae species. *Sci. Total Environ.* **2015**, *518*, 217–224. [[CrossRef](#)] [[PubMed](#)]
40. Melegari, S.P.; Perreault, F.; Costa, R.H.R.; Popovic, R.; Matias, W.G. Evaluation of toxicity and oxidative stress induced by copper oxide nanoparticles in the green alga *Chlamydomonas reinhardtii*. *Aquat. Toxicol.* **2013**, *142*, 431–440. [[CrossRef](#)] [[PubMed](#)]
41. Aruoja, V.; Dubourguier, H.-C.; Kasemets, K.; Kahru, A. Toxicity of nanoparticles of CuO, ZnO and TiO₂ to microalgae *Pseudokirchneriella subcapitata*. *Sci. Total Environ.* **2009**, *407*, 1461–1468. [[CrossRef](#)]
42. Schwab, F.; Bucheli, T.D.; Lukhele, L.P.; Magrez, A.; Nowack, B.; Sigg, L.; Knauer, K. Are carbon nanotube effects on green algae caused by shading and agglomeration? *Environ. Sci. Technol.* **2011**, *45*, 6136–6144. [[CrossRef](#)]
43. Wang, Z.; Li, J.; Zhao, J.; Xing, B. Toxicity and internalization of CuO nanoparticles to prokaryotic alga microcystis aeruginosa as affected by dissolved organic matter. *Environ. Sci. Technol.* **2011**, *45*, 6032–6040. [[CrossRef](#)]
44. Zhao, J.; Cao, X.; Liu, X.; Wang, Z.; Zhang, C.; White, J.C.; Xing, B. Interactions of CuO nanoparticles with the algae *Chlorella pyrenoidosa*: Adhesion, uptake, and toxicity. *Nanotoxicology* **2016**, *10*, 1297–1305. [[CrossRef](#)]
45. Navarro, E.; Piccapietra, F.; Wagner, B.; Marconi, F.; Kaegi, R.; Odzak, N.; Sigg, L.; Behra, R. Toxicity of silver nanoparticles to *Chlamydomonas reinhardtii*. *Environ. Sci. Technol.* **2008**, *42*, 8959–8964. [[CrossRef](#)]
46. Bondarenko, O.M.; Heinlaan, M.; Sihtmäe, M.; Ivask, A.; Kurvet, I.; Joonas, E.; Jemec, A.; Mannerstrom, M.; Heinonen, T.; Rekulapelly, R.; et al. Multilaboratory evaluation of 15 bioassays for (eco)toxicity screening and hazard ranking of engineered nanomaterials: FP7 project NANOVALID. *Nanotoxicology* **2016**, *10*, 1229–1242. [[CrossRef](#)]
47. Samei, M.; Sarrafzadeh, M.-H.; Faramarzi, M.A. The impact of morphology and size of zinc oxide nanoparticles on its toxicity to the freshwater microalga, *Raphidocelis subcapitata*. *Environ. Sci. Pollut. Res.* **2019**, *26*, 2409–2420. [[CrossRef](#)]
48. Aravantinou, A.F.; Andreou, F.; Manariotis, I.D. Long-term toxicity of ZnO nanoparticles to *Scenedesmus rubescens* cultivated in different media. *Sci. Rep.* **2017**, *7*, 13454. [[CrossRef](#)] [[PubMed](#)]
49. Zhang, C.; Wang, J.; Tan, L.; Chen, X. Toxic effects of nano-ZnO on marine microalgae *Skeletonema costatum*: Attention to the accumulation of intracellular Zn. *Aquat. Toxicol.* **2016**, *178*, 158–164. [[CrossRef](#)] [[PubMed](#)]
50. Juganson, K.; Ivask, A.; Blinova, I.; Mortimer, M.; Kahru, A. NanoE-Tox: New and in-depth database concerning ecotoxicity of nanomaterials. *Beilstein J. Nanotechnol.* **2015**, *6*, 1788–1804. [[CrossRef](#)] [[PubMed](#)]
51. Vandebriel, R.J.; Vermeulen, J.P.; van Engelen, L.B.; de Jong, B.; Verhagen, L.M.; de la Fonteyne-Blankestijn, L.J.; Hoonakker, M.E.; de Jong, W.H. The crystal structure of titanium dioxide nanoparticles influences immune activity in vitro and in vivo. *Part. Fibre Toxicol.* **2018**, *15*, 9. [[CrossRef](#)] [[PubMed](#)]
52. Van Hoecke, K.; De Schamphelaere, K.A.C.; Van der Meeren, P.; Lucas, S.; Janssen, C.R. Ecotoxicity of silica nanoparticles to the green alga *pseudokirchneriella subcapitata*: Importance of surface area. *Environ. Toxicol. Chem.* **2009**, *27*, 1948–1957. [[CrossRef](#)]
53. Yu, Z.; Hao, R.; Zhang, L.; Zhu, Y. Effects of TiO₂, SiO₂, Ag and CdTe/CdS quantum dots nanoparticles on toxicity of cadmium towards *Chlamydomonas reinhardtii*. *Ecotoxicol. Environ. Saf.* **2018**, *156*, 75–86. [[CrossRef](#)]
54. Perales-Vela, H.V.; González-Moreno, S.; Montes-Horcasitas, C.; Cañizares-Villanueva, R.O. Growth, photosynthetic and respiratory responses to sub-lethal copper concentrations in *Scenedesmus incrassatulus* (Chlorophyceae). *Chemosphere* **2007**, *67*, 2274–2281. [[CrossRef](#)]
55. Perreault, F.; Popovic, R.; Dewez, D. Different toxicity mechanisms between bare and polymer-coated copper oxide nanoparticles in *Lemna gibba*. *Environ. Pollut.* **2014**, *185*, 219–227. [[CrossRef](#)]

56. Perreault, F.; Samadani, M.; Dewez, D. Effect of soluble copper released from copper oxide nanoparticles solubilisation on growth and photosynthetic processes of *Lemna gibba* L. *Nanotoxicology* **2014**, *8*, 374–382. [[CrossRef](#)]
57. Yue, L.; Zhao, J.; Yu, X.; Lv, K.; Wang, Z.; Xing, B. Interaction of CuO nanoparticles with duckweed (*Lemna minor* L.): Uptake, distribution and ROS production sites. *Environ. Pollut.* **2018**, *243*, 543–552. [[CrossRef](#)]
58. Shi, J.; Abid, A.D.; Kennedy, I.M.; Hristova, K.R.; Silk, W.K. To duckweeds (*Landoltia punctata*), nanoparticulate copper oxide is more inhibitory than the soluble copper in the bulk solution. *Environ. Pollut.* **2011**, *159*, 1277–1282. [[CrossRef](#)] [[PubMed](#)]
59. Hu, C.; Liu, Y.; Li, X.; Li, M. Biochemical responses of duckweed (*Spirodela polyrhiza*) to zinc oxide nanoparticles. *Arch. Environ. Contam. Toxicol.* **2013**, *64*, 643–651. [[CrossRef](#)] [[PubMed](#)]
60. Chen, X.; O'Halloran, J.; Jansen, M.A.K. The toxicity of zinc oxide nanoparticles to *Lemna minor* (L.) is predominantly caused by dissolved Zn. *Aquat. Toxicol.* **2016**, *174*, 46–53. [[CrossRef](#)] [[PubMed](#)]
61. Schoelynck, J.; Bal, K.; Backx, H.; Okruszko, T.; Meire, P.; Struyf, E. Silica uptake in aquatic and wetland macrophytes: A strategic choice between silica, lignin and cellulose? *New Phytol.* **2010**, *186*, 385–391. [[CrossRef](#)]
62. Wu, F.; Harper, B.J.; Harper, S.L. Comparative dissolution, uptake, and toxicity of zinc oxide particles in individual aquatic species and mixed populations. *Environ. Toxicol. Chem.* **2019**, *38*, 591–602. [[CrossRef](#)] [[PubMed](#)]
63. Hund-Rinke, K.; Simon, M. Ecotoxic effect of photocatalytic active nanoparticles (TiO₂) on algae and daphnids (8 pp). *Environ. Sci. Pollut. Res.* **2006**, *13*, 225–232. [[CrossRef](#)] [[PubMed](#)]
64. Xiao, Y.; Vijver, M.G.; Chen, G.; Peijnenburg, W.J.G.M. Toxicity and accumulation of Cu and ZnO nanoparticles in *Daphnia magna*. *Environ. Sci. Technol.* **2015**, *49*, 4657–4664. [[CrossRef](#)]
65. Novak, S.; Jemec Kokalj, A.; Hočevár, M.; Godec, M.; Drobne, D. The significance of nanomaterial post-exposure responses in *Daphnia magna* standard acute immobilisation assay: Example with testing TiO₂ nanoparticles. *Ecotoxicol. Environ. Saf.* **2018**, *152*, 61–66. [[CrossRef](#)]
66. Posthuma, L.; Suter, G.W., II; Tras, T.P. *Species Sensitivity Distribution in Ecotoxicology*; CRC/Lewis: Boca Raton, FL, USA, 2002.
67. Adam, N.; Vakurov, A.; Knapen, D.; Blust, R. The chronic toxicity of CuO nanoparticles and copper salt to *Daphnia magna*. *J. Hazard. Mater.* **2015**, *283*, 416–422. [[CrossRef](#)]
68. Kim, S.; Samanta, P.; Yoo, J.; Kim, W.-K.; Jung, J. Time-dependent toxicity responses in *Daphnia magna* exposed to CuO and ZnO nanoparticles. *Bull. Environ. Contam. Toxicol.* **2017**, *98*, 502–507. [[CrossRef](#)]
69. Muna, M.; Blinova, I.; Kahru, A.; Vrčec, I.V.; Pem, B.; Orupöld, K.; Heinlaan, M. Combined effects of test media and dietary algae on the toxicity of CuO and ZnO nanoparticles to freshwater microcrustaceans *Daphnia magna* and *Heterocypris incongruens*: Food for thought. *Nanomaterials* **2019**, *9*, 23. [[CrossRef](#)] [[PubMed](#)]
70. Rossetto, A.L.d.O.F.; Melegari, S.P.; Ouriques, L.C.; Matias, W.G. Comparative evaluation of acute and chronic toxicities of CuO nanoparticles and bulk using *Daphnia magna* and *Vibrio fischeri*. *Sci. Total Environ.* **2014**, *490*, 807–814. [[CrossRef](#)] [[PubMed](#)]
71. Santo, N.; Fascio, U.; Torres, F.; Guazzoni, N.; Tremolada, P.; Bettinetti, R.; Mantecca, P.; Bacchetta, R. Toxic effects and ultrastructural damages to *Daphnia magna* of two differently sized ZnO nanoparticles: Does size matter? *Water Res.* **2014**, *53*, 339–350. [[CrossRef](#)] [[PubMed](#)]
72. Lin, L.; Xu, M.; Mu, H.; Wang, W.; Sun, J.; He, J.; Qiu, J.-W.; Luan, T. Quantitative proteomic analysis to understand the mechanisms of zinc oxide nanoparticle toxicity to *Daphnia pulex* (Crustacea: Daphniidae): Comparing with bulk zinc oxide and zinc salt. *Environ. Sci. Technol.* **2019**, *53*, 5436–5444. [[CrossRef](#)]
73. Heinlaan, M.; Ivask, A.; Blinova, I.; Dubourguier, H.-C.; Kahru, A. Toxicity of nanosized and bulk ZnO, CuO and TiO₂ to bacteria *Vibrio fischeri* and crustaceans *Daphnia magna* and *Thamnocephalus platyurus*. *Chemosphere* **2008**, *71*, 1308–1316. [[CrossRef](#)]
74. Iswarya, V.; Sharma, V.; Chandrasekaran, N.; Mukherjee, A. Impact of tetracycline on the toxic effects of titanium dioxide (TiO₂) nanoparticles towards the freshwater algal species, *Scenedesmus obliquus*. *Aquat. Toxicol.* **2017**, *193*, 168–177. [[CrossRef](#)]
75. Sadiq, I.M.; Dalai, S.; Chandrasekaran, N.; Mukherjee, A. Ecotoxicity study of titania (TiO₂) NPs on two microalgae species: *Scenedesmus* sp. and *Chlorella* sp. *Ecotoxicol. Environ. Saf.* **2011**, *74*, 1180–1187. [[CrossRef](#)]
76. Iswarya, V.; Bhuvaneshwari, M.; Chandrasekaran, N.; Mukherjee, A. Individual and binary toxicity of anatase and rutile nanoparticles towards *Ceriodaphnia dubia*. *Aquat. Toxicol.* **2016**, *178*, 209–221. [[CrossRef](#)]
77. Nicolas, M.; Séverine, L.M.; Anne, B.-N.; Pascal, P. Effect of two TiO₂ nanoparticles on the growth of unicellular green algae using the OECD 201 test guideline: Influence of the exposure system. *Toxicol. Environ. Chem.* **2016**, *98*, 860–876. [[CrossRef](#)]
78. Zhu, X.; Zhu, L.; Chen, Y.; Tian, S. Acute toxicities of six manufactured nanomaterial suspensions to *Daphnia magna*. *J. Nanoparticle Res.* **2009**, *11*, 67–75. [[CrossRef](#)]
79. Ude, V.C.; Brown, D.M.; Viale, L.; Kanase, N.; Stone, V.; Johnston, H.J. Impact of copper oxide nanomaterials on differentiated and undifferentiated Caco-2 intestinal epithelial cells; assessment of cytotoxicity, barrier integrity, cytokine production and nanomaterial penetration. *Part. Fibre Toxicol.* **2017**, *14*, 31. [[CrossRef](#)] [[PubMed](#)]
80. Piret, J.-P.; Vankoningsloo, S.; Mejia, J.; Noël, F.; Boilan, E.; Lambinon, F.; Zouboulis, C.C.; Masereel, B.; Lucas, S.; Saout, C.; et al. Differential toxicity of copper (II) oxide nanoparticles of similar hydrodynamic diameter on human differentiated intestinal Caco-2 cell monolayers is correlated in part to copper release and shape. *Nanotoxicology* **2012**, *6*, 789–803. [[CrossRef](#)] [[PubMed](#)]
81. Piret, J.-P.; Jacques, D.; Audinot, J.-N.; Mejia, J.; Boilan, E.; Noël, F.; Fransolet, M.; Demazy, C.; Lucas, S.; Saout, C.; et al. Copper (II) oxide nanoparticles penetrate into HepG2 cells, exert cytotoxicity via oxidative stress and induce pro-inflammatory response. *Nanoscale* **2012**, *4*, 7168–7184. [[CrossRef](#)] [[PubMed](#)]

82. Luo, C.; Li, Y.; Yang, L.; Zheng, Y.; Long, J.; Jia, J.; Xiao, S.; Liu, J. Activation of Erk and p53 regulates copper oxide nanoparticle-induced cytotoxicity in keratinocytes and fibroblasts. *Int. J. Nanomed.* **2014**, *9*, 4763–4772. [[CrossRef](#)]
83. Karlsson, H.L.; Cronholm, P.; Gustafsson, J.; Möller, L. Copper oxide nanoparticles are highly toxic: A comparison between metal oxide nanoparticles and carbon nanotubes. *Chem. Res. Toxicol.* **2008**, *21*, 1726–1732. [[CrossRef](#)]
84. Abbott, C.T.E.; Schwab, K.J. Toxicity of commercially available engineered nanoparticles to Caco-2 and SW480 human intestinal epithelial cells. *Cell Biol. Toxicol.* **2013**, *29*, 101–116. [[CrossRef](#)]
85. Abbasi-Oshaghi, E.; Mirzaei, F.; Mirzaei, A. Effects of ZnO nanoparticles on intestinal function and structure in normal/high fat diet-fed rats and Caco-2 cells. *Nanomedicine* **2018**, *13*, 2791–2816. [[CrossRef](#)]
86. Sharma, V.; Anderson, D.; Dhawan, A. Zinc oxide nanoparticles induce oxidative DNA damage and ROS-triggered mitochondria mediated apoptosis in human liver cells (HepG2). *Apoptosis* **2012**, *17*, 852–870. [[CrossRef](#)]
87. Vinardell, M.P.; Llanas, H.; Marics, L.; Montserrat, M. In Vitro comparative skin irritation induced by nano and non-nano zinc oxide. *Nanomaterials* **2017**, *7*, 56. [[CrossRef](#)]
88. Lee, S.H.; Lee, H.R.; Kim, Y.-R.; Kim, M.-K. Toxic response of zinc oxide nanoparticles in human epidermal keratinocyte HaCaT cells. *Toxicol. Environ. Health Sci.* **2012**, *4*, 14–18. [[CrossRef](#)]
89. Song, W.; Zhang, J.; Guo, J.; Zhang, J.; Ding, F.; Li, L.; Sun, Z. Role of the dissolved zinc ion and reactive oxygen species in cytotoxicity of ZnO nanoparticles. *Toxicol. Lett.* **2010**, *199*, 389–397. [[CrossRef](#)] [[PubMed](#)]
90. Heng, B.C.; Zhao, X.; Xiong, S.; Woei, N.K.; Boey, F.Y.-C.; Loo, J.S.-C. Toxicity of zinc oxide (ZnO) nanoparticles on human bronchial epithelial cells (BEAS-2B) is accentuated by oxidative stress. *Food Chem. Toxicol.* **2010**, *48*, 1762–1766. [[CrossRef](#)] [[PubMed](#)]
91. Johnson, B.M.; Fraietta, J.A.; Gracias, D.T.; Hope, J.L.; Stairiker, C.J.; Patel, P.R.; Mueller, Y.M.; McHugh, M.D.; Jablonowski, L.J.; Wheatley, M.A.; et al. Acute exposure to ZnO nanoparticles induces autophagic immune cell death. *Nanotoxicology* **2015**, *9*, 737–748. [[CrossRef](#)] [[PubMed](#)]
92. Tada-Oikawa, S.; Ichihara, G.; Fukatsu, H.; Shimanuki, Y.; Tanaka, N.; Watanabe, E.; Suzuki, Y.; Murakami, M.; Izuoka, K.; Chang, J.; et al. Titanium dioxide particle type and concentration influence the inflammatory response in Caco-2 cells. *Int. J. Mol. Sci.* **2016**, *17*, 576. [[CrossRef](#)]
93. Wang, Y.; Aker, W.G.; Hwang, H.; Yedjou, C.G.; Yu, H.; Tchounwou, P.B. A study of the mechanism of in vitro cytotoxicity of metal oxide nanoparticles using catfish primary hepatocytes and human HepG2 cells. *Sci. Total Environ.* **2011**, *409*, 4753–4762. [[CrossRef](#)]
94. Bessa, M.J.; Costa, C.; Reinoso, J.; Pereira, C.; Fraga, S.; Fernández, J.; Bañares, M.A.; Teixeira, J.P. Moving into advanced nanomaterials. Toxicity of rutile TiO₂ nanoparticles immobilized in nanokaolin nanocomposites on HepG2 cell line. *Toxicol. Appl. Pharmacol.* **2017**, *316*, 114–122. [[CrossRef](#)]
95. Allouni, Z.E.; Cimpan, M.R.; Høl, P.J.; Skodvin, T.; Gjerdet, N.R. Agglomeration and sedimentation of TiO₂ nanoparticles in cell culture medium. *Colloids Surf. B* **2009**, *68*, 83–87. [[CrossRef](#)]
96. Murugadoss, S.; Lison, D.; Godderis, L.; Van Den Brule, S.; Mast, J.; Brassinne, F.; Sebaihi, N.; Hoet, P.H. Toxicology of silica nanoparticles: An update. *Arch. Toxicol.* **2017**, *91*, 2967–3010. [[CrossRef](#)]
97. Ahmad, J.; Ahamed, M.; Akhtar, M.J.; Alrokayan, S.A.; Siddiqui, M.A.; Musarrat, J.; Al-Khedhairy, A.A. Apoptosis induction by silica nanoparticles mediated through reactive oxygen species in human liver cell line HepG2. *Toxicol. Appl. Pharmacol.* **2012**, *259*, 160–168. [[CrossRef](#)]
98. Gong, C.; Yang, L.; Zhou, J.; Guo, X.; Zhuang, Z. Possible role of PAPR-1 in protecting human HaCaT cells against cytotoxicity of SiO₂ nanoparticles. *Toxicol. Lett.* **2017**, *280*, 213–221. [[CrossRef](#)]
99. Liang, H.; Jin, C.; Tang, Y.; Wang, F.; Ma, C.; Yang, Y. Cytotoxicity of silica nanoparticles on HaCaT cells. *J. Appl. Toxicol.* **2014**, *34*, 367–372. [[CrossRef](#)] [[PubMed](#)]
100. Li, Y.; Sun, L.; Jin, M.; Du, Z.; Liu, X.; Guo, C.; Li, Y.; Huang, P.; Sun, Z. Size-dependent cytotoxicity of amorphous silica nanoparticles in human hepatoma HepG2 cells. *Toxicol. Vitro.* **2011**, *25*, 1343–1352. [[CrossRef](#)] [[PubMed](#)]
101. Krug, H.F. Nanosafety research—Are we on the right track? *Angew. Chem. Int. Ed.* **2014**, *53*, 12304–12319.